



**HAL**  
open science

# Mixed Light and Biocide Pollution Affects Lipid Profiles of Periphyton Communities in Freshwater Ecosystems

Nicolas Mazzella, Romain Vrba, Aurélie Moreira, Nicolas Creusot, Mélissa Eon, Débora Millan-Navarro, Isabelle Lavoie, Soizic Morin

## ► To cite this version:

Nicolas Mazzella, Romain Vrba, Aurélie Moreira, Nicolas Creusot, Mélissa Eon, et al.. Mixed Light and Biocide Pollution Affects Lipid Profiles of Periphyton Communities in Freshwater Ecosystems. 2023. hal-04173358

**HAL Id: hal-04173358**

**<https://hal.inrae.fr/hal-04173358v1>**

Preprint submitted on 31 Jul 2023

**HAL** is a multi-disciplinary open access archive for the deposit and dissemination of scientific research documents, whether they are published or not. The documents may come from teaching and research institutions in France or abroad, or from public or private research centers.

L'archive ouverte pluridisciplinaire **HAL**, est destinée au dépôt et à la diffusion de documents scientifiques de niveau recherche, publiés ou non, émanant des établissements d'enseignement et de recherche français ou étrangers, des laboratoires publics ou privés.

1 **Mixed light and biocide pollution affects lipid profiles of**  
2 **periphyton communities in freshwater ecosystems**

3  
4 Nicolas MAZZELLA<sup>1\*</sup>, Romain VRBA<sup>1,2</sup>, Aurélie MOREIRA<sup>1</sup>, Nicolas CREUSOT<sup>1</sup>,  
5 Mélissa EON<sup>1</sup>, Débora MILLAN-NAVARRO<sup>1</sup>, Isabelle LAVOIE<sup>2</sup>, Soizic MORIN<sup>1</sup>

6  
7 <sup>1</sup> INRAE, UR EABX, 50 avenue de Verdun, 33612 Cestas cedex, France

8 <sup>2</sup> INRS-ETE, 490 rue de la Couronne, Québec, QC G1K 9A9, Canada

9 \*Corresponding author at: INRAE, UR EABX, 50 avenue de Verdun, 33612 Cestas cedex, France.

10  
11  
12 **Highlights**

- 13  
14 • BAC 12 exposure leads to glycolipid disappearance and a drastic decrease in PUFAs,  
15 indicating noticeable impacts on phototrophic organisms within the biofilm.  
16 • The information provided by the fatty acids deduced from polar lipids did not allow  
17 decoupling the effect of light conditions from BAC 12 exposure.  
18 • In contrast, lipid molecular species analysis could show an increase in green algae and  
19 cyanobacteria when compared to diatoms under the effect of photoperiod.  
20 • It may also be proposed that certain molecular species, particularly those from PCs and  
21 DGDGs, might act as more accurate biofilm-scale markers of light duration.  
22  
23

24 **Abstract**

25

26 The composition of lipids in algae are significantly influenced by environmental factors,  
27 including light intensity. Exposure to organic and inorganic contaminants can also disrupt the  
28 synthesis of fatty acids, changing the lipid composition of microalgae in periphytic  
29 communities. In this study, we looked at how a biocide such as  
30 dodecylbenzyltrimethylammonium chloride (BAC 12) and two photoperiod durations can affect  
31 a biofilm's polar lipidome in a microcosm experiment. The heterotrophic compartment  
32 appeared to be raised by exposure to BAC 12 at the expense of phototrophic organisms.  
33 Additionally, the overall decline in polyunsaturated fatty acids indicated that the biofilm's  
34 phototrophic organisms were all severely impacted. However, it may be difficult to differentiate  
35 the effects of contamination from those of light, since there was no observable effect of  
36 photoperiods on the conventional fatty acid determination. The molecular species composition  
37 of both glycolipids and phospholipids was investigated in additional multivariate analyses. It  
38 was suggested that some molecular species may serve as more specific markers of light duration  
39 at the biofilm scale. Lastly, we recommend applying a similar lipidomic approach with  
40 monospecific cultures of microalgal strains in future research to support these findings, as the  
41 methodology used in this study would be applicable to other biofilm-derived microorganisms.

42 **Keywords**

43 Artificial light at night, quaternary ammonium compound, biofilm, microalgae, lipidomics,  
44 fatty acids.

45

## 46 1. Introduction

47

48 Freshwater biofilms are composed of a large variety of microorganisms, covering all  
49 kingdoms of life (bacteria, archaea, fungi, plantae, protista and animalia). Lipids can be  
50 considered as markers of the structure of a community of microorganisms. Fatty acids in  
51 autotrophic organisms, such as diatoms, green algae, cyanobacteria, and fungi, have distinct  
52 lipid profiles. Diatoms primarily consist of 14-, 16-, and 20-carbon saturated and unsaturated  
53 fatty acids (FA), while they produce minor or negligible 18-carbon FAs (Opute 1974).  
54 Chlorophyceae and cyanophyceae produce more octadecadienoic and octadecatrienoic fatty  
55 acids, while green algae produce hexadecatrienoic and hexadecatetraenoic acids more  
56 significantly (Zäuner et al. 2012). Thylakoid membranes in algae mainly consist of glycolipids,  
57 while phospholipids like phosphatidylethanolamine (PE), phosphatidylcholine (PC) and  
58 phosphatidylglycerol (PG) are less specific due to their presence in both microalgae and  
59 prokaryotic cells (Zulu et al. 2018, Li-Beisson et al. 2019). Algal lipid content is also strongly  
60 influenced by environmental factors. For instance, at low temperatures, the degree of  
61 unsaturation increases to maintain membrane fluidity and integrity, leading to an increase in  
62 polyunsaturated fatty-acids (PUFA) compared to saturated fatty-acids (SFA) and monosaturated  
63 fatty-acids (MUFA) (Fuschino et al. 2011). Light conditions are also known to affect lipid  
64 composition in algae. As lipids are important components of thylakoid membranes, they are  
65 involved in the regulation of photosynthetic capacity (Wacker et al. 2015). Lastly, exposure to  
66 organic and inorganic contaminants can likewise interfere with fatty acid synthesis, leading to  
67 a change in algae and biofilm lipid content (Robert et al. 2007, Filimonova et al. 2016,  
68 Fadhlaoui et al. 2020). Recent works have focused on fatty acids as algal biomarkers of  
69 environmental stress because their composition is very sensitive to stressors and environmental  
70 modifications (Arts et al. 2001, Demailly et al. 2019). However, the combined effects of

71 stressors in an urban environment and the subsequent reactions of microorganisms within  
72 biofilms remain poorly understood. An earlier research aimed at determining the individual and  
73 combined effects of urban stressors, namely dodecylbenzyltrimethylammonium chloride (BAC  
74 12) contaminant and Artificial Light at Night (ALAN) on autotrophic organisms in the biofilm  
75 (Vrba et al. 2023). This previous work revealed the predominant effects of the biocidal activity  
76 on autotrophic organisms in the environment, both at the scale of algal group (i.e., green algae,  
77 diatoms and cyanobacteria) and at the level of photosynthetic response. The evolution of major  
78 lipid classes, including phospholipids such as PE, PC and PG, glycolipids such as  
79 monogalactosyldiacylglycerol (MGDG), digalactosyldiacylglycerol (DGDG) and  
80 sulfoquinovosyldiacylglycerol (SQDG) was also determined. These previous results are  
81 complemented here by the determination of the molecular species composition within PE, PC,  
82 PG, MGDG and DGDG classes. Identification and quantification of the molecular species also  
83 allowed estimation of the major fatty acid fractions. More precisely, the following study will  
84 (i) address the effects of BAC 12 on the fatty acid composition of polar lipids through the study  
85 of molecular species, and (ii) discuss the possible effect of light (i.e., alternating or continuous  
86 photoperiod) that seemed difficult to uncouple from the strong and overlapping effect of the  
87 biocide.

88

89

## 2. Experimental section

### 2.1. Chemicals and reagents

The following polar lipid standards were purchased from Avanti Polar Lipids: 1-palmitoyl-2-oleoyl-glycerol-3-phosphocholine or PC (16:0/18:1) (850457), 1-palmitoyl-2-oleoyl-sn-glycerol-3-phosphoethanolamine or PE (16:0/18:1) (850757), 1-palmitoyl-2-oleoyl-sn-glycerol-3-phospho-(1'-rac-glycerol) or PG (16:0/18:1) (840457), 1,2-diheptadecanoyl-sn-glycerol-3-phosphocholine or PC (17:0/17:0) (850360), 1,2-diheptadecanoyl-sn-glycerol-3-phosphoethanolamine or PE (17:0/17:0) (830756), 1,2-dipentadecanoyl-sn-glycerol-3-phosphoethanolamine or PE (15:0/15:0) (850704), and 1,2-diheptadecanoyl-sn-glycerol-3-phospho-(1'-rac-glycerol) or PG (17:0/17:0) (830456), L- $\alpha$ -phosphatidylserine (Soy, 99%) (sodium salt) (870336) for the phospholipid standards, and monogalactosyldiacylglycerol (840523), digalactosyldiacylglycerol (840524) and sulfoquinovosyldiacylglycerol (840525) from plant extracts as glycolipid standards. Ammonium acetate (LiChropur) were provided by Sigma-Aldrich. Palmitic acid (76119), oleic acid (O1008), heptadecanoic acid (H3500) and eicosapentanoic acid (44864) analytical standard grades (purity $\geq$ 98 %) were purchased from Sigma-Aldrich. Acetonitrile, methanol (MeOH) tert-Butyl methyl ether (MTBE) and isopropanol HPLC grades were purchased from Biosolve Chimie, France. Ultrapure water (UPW) was obtained from Direct-Q<sup>®</sup> Water Purification System (Merck Millipore). Dodecylbenzyltrimethylammonium chloride (BAC 12, purity $\geq$ 99 %) and Benzyl-2,3,4,5,6-d<sub>5</sub>-dimethyl-n-dodecylammonium chloride (purity $>$ 98 %) were obtained from Sigma-Aldrich and Cluzeau (France), respectively.

### 2.2. Experimental design

Glass slides (individual surface area: 150 cm<sup>2</sup>) were placed in a small hypertrophic pond in Cestas (Bordeaux, France)(Chaumet et al. 2019) for colonization by microbial biofilms.

115 After five months, colonized substrates were removed from the natural environment and were  
116 randomly placed in experimental channels (on day 0 = T0) under laboratory conditions as  
117 described in Vrba et al. (2023). Briefly, four experimental conditions were set up, each in  
118 pseudo-triplicates (i.e., separate 10-L channels fed by a common 10-L tank). The tanks and  
119 channels were filled with filtered (20  $\mu\text{m}$ ) pond water, at a room temperature of  $20.5 \pm 0.1^\circ\text{C}$   
120 and water temperature of  $18.7 \pm 0.2^\circ\text{C}$ . The four conditions were as follow: two treatments  
121 under uncontaminated conditions (controls, CTRL) and two treatments exposed to  $30 \text{ mg L}^{-1}$   
122 of BAC 12 (BAC). All channels were exposed either to normal light (NL) corresponding to a  
123 14h day/10h night photoperiod ( $20 \mu\text{mol m}^{-2} \text{ s}^{-1}$ ) or to continuous light (CL). Treatments will  
124 be referred as CTRL-NL, CTRL-CL, BAC-NL and BAC-CL. On day 0, biofilms were collected  
125 to assess their initial lipid composition, prior to exposure to either BAC or CL. On day 10 (T10),  
126 biofilms were collected to analyse qualitative and quantitative changes in lipid profiles.  
127 Biofilms were immediately quenched in liquid nitrogen, and then collected by scraping the  
128 glass slides with a razor blade. The samples were freeze-dried (Benchtop Ro 8LZL BTF) and  
129 kept at  $-80^\circ\text{C}$  until the extraction step.

### 130 **2.3. Nutrient and BAC12 dosing in exposure water**

131 Nutrients and mineral salts were monitored and analyzed using a Metrohm 881 Compact  
132 Ionic Chromatograph pro (Metrohm). Anion analysis ( $\text{PO}_4^-$ ,  $\text{NO}_3^-$ ,  $\text{NO}_2^-$ ,  $\text{Cl}^-$  and  $\text{SO}_4^{2-}$ ) was  
133 performed using a Supp 4/5 Guard/4.0 precolumn followed by a Metrosep A Supp5 – 250/4.0  
134 column. The mobile phase was a mixture of a solution of  $3.2 \text{ mmol L}^{-1} \text{ Na}_2\text{CO}_3$  and a solution  
135 of  $1 \text{ mmol L}^{-1} \text{ NaHCO}_3$ . Cation analysis ( $\text{Na}^+$ ,  $\text{K}^+$ ,  $\text{Ca}^{2+}$ ,  $\text{Mg}^{2+}$  and  $\text{NH}_4^+$ ) was performed using  
136 a C4 Guard/4.0 precolumn followed by a Metrosep C6 - 250/4.0 column). The eluent used was  
137 a mixture of  $2.5 \text{ mmol L}^{-1} \text{ HNO}_3$  and a solution of  $1.7 \text{ mmol L}^{-1}$  10,12-Pentacosadynoic acid  
138 (PCDA). Calibration ranges were from 20 to  $1000 \mu\text{g.L}^{-1}$ . BAC 12 concentrations in the water  
139 were monitored at the beginning (T0) and the end of experiment (T10). Three samples of 20

140 mL were collected from each channel and stored at  $-20^{\circ}\text{C}$  together with the stock solution until  
141 analysis. The samples were analyzed using an Ultimate 3000 HPLC coupled with an API 2000  
142 triple quadrupole mass spectrometer. A Gemini® NX-C18 column (Phenomenex) was used as  
143 a stationary phase. The mobile phase was 90:10 (5 mM ammonium acetate:acetonitrile, v/v).  
144 The chromatographic separation was done in isocratic mode with a flow rate of  $0.6\text{ mL min}^{-1}$ .  
145 The injection volume was set at  $20\ \mu\text{L}$ . An internal standard of benzyl-2,3,4,5,6- $\text{d}_5$ -dimethyl-  
146 n-dodecylammonium chloride was used, and its concentration in sample vials was typically  $100$   
147  $\text{ng mL}^{-1}$ . Samples were diluted and the calibration range was from 1 to  $200\ \mu\text{g L}^{-1}$ . Quality  
148 controls were regularly injected at concentrations of 5 and  $25\ \mu\text{g L}^{-1}$ , as well as analytical  
149 blanks. Concentration values for either BAC 12 (Table A 1) or nutrients are available in Vrba  
150 et al. (2023).

#### 151 **2.4. Lipid extraction**

152 The biofilm samples (10-20 mg of dry mass) were weighed using a Mettler Toledo  
153 NS204S precision balance and placed in 2 mL microtubes with 150 mg of microbeads. The  
154 biphasic extraction procedure involved addition of 1 mL of a MTBE:MeOH (3:1, v/v) mixture  
155 and  $650\ \mu\text{L}$  of a UPW:MeOH (3:1, v/v) mixture. Prior to extraction,  $50\ \mu\text{L}$  of a PE (15:0/15:0)  
156 solution containing  $100\ \text{ng mL}^{-1}$  was added as a surrogate. Samples containing microbeads were  
157 mechanically homogenized and extracted (3 cycles of 15 s) with the solvent mixtures by using  
158 a MP Biomedicals FastPrep-24 5G. The upper lipophilic phase (MTBE) was separated from  
159 the lower hydrophilic phase (UPW and MeOH) by centrifugation at 12,000 RPM.  $600\ \mu\text{L}$  of  
160 the lipophilic phase was collected. A second extraction step extracted (3 cycles of 15 s) was  
161 carried out after adding  $700\ \mu\text{L}$  of MTBE:MeOH mixture 3:1 (v/v) and  $455\ \mu\text{L}$  UPW:MeOH  
162 mixture 3:1 (v/v). The supernatant (MTBE) was collected again and added to the previous one.  
163 Only organic lipophilic phases (1.1 mL) were kept for further polar lipid analysis. Extracts were  
164 stored at  $-80^{\circ}\text{C}$  and solvent underwent extraction as a procedural blank to verify the absence of



165 contamination during extracting procedures. Further details regarding the whole extraction  
166 procedure can be found in Mazzella et al. (2023b). The samples were then diluted in appropriate  
167 solvent injection (typical volume of 1 mL) and stored at -18°C until analysis within one week.

## 168 **2.5. HPLC-ESI-MS/MS analysis**

169 Lipid extracts were also analyzed with a Dionex Ultimate 3000 HPLC (Thermo Fisher  
170 Scientific, France) coupled with an API 2000 triple quadrupole mass spectrometer (Sciex,  
171 France). Chromatographic separation of both glycolipids and phospholipids was performed on  
172 a Luna NH<sub>2</sub> HILIC column (3 μm, 100 × 2 mm) with a Security Guard cartridge NH<sub>2</sub> (4 × 2.0  
173 mm). The injection volume and temperature were set to 20 μL and 40°C, respectively. The  
174 chromatographic separation and mass spectrometry conditions are described in Mazzella et al.  
175 (2023a), (2023b). Quantitation of phosphatidylcholine (PC), phosphatidylethanolamine (PE)  
176 and phosphatidylglycerol (PG) were respectively carried out with: PC (16:0/18:1), PE  
177 (16:0/18:1), PG (16:0/18:1). Quantitation of glycolipids was carried out with MGDG  
178 (16:3\_18:3) (63 % of the total MGDG standard), DGDG (18:3/18:3) (22 % of the total MGDG  
179 standard), and SQDG (34:3) (78 % of the total SQDG standard). The internal standards utilized  
180 were PC (17:0/17:0) for PC phospholipids, PE (17:0/17:0) for PE phospholipids and both  
181 MGDG and DGDG glycolipids, and PG (17:0/17:0) for PG and SQDG. Concentrations for both  
182 phospholipids and glycolipids were reported in nmol mg<sup>-1</sup> (dry weight), and the limits of  
183 quantification were typically between 0.02-0.05 nmol mg<sup>-1</sup>, depending on analyte response.

184 In addition to intact lipids, free fatty acids were analyzed by RPLC-ESI-MS/MS using  
185 the same analytical equipment. However, in that case, chromatographic separation was  
186 performed on a Kinetex C8 column (2.8 μm, 100 x 2.1 mm). Heptadecanoic acid (C17:0) was  
187 used here as an internal standard. Finally, the chromatographic and acquisition parameters are  
188 given in the appendices (Table A 2 and Table A 3).

## 189 2.6. Phospholipid and glycolipid nomenclatures

190 Polar glycerolipids are constituted of a glycerol backbone esterified by two fatty acids  
191 on the sn-1 and sn-2 positions. The moiety linked to the sn-3 position refers to the polar head  
192 group (e.g., sn-phospho-3-glycerol for the PG, a  $\beta$ -D-galactosyl group for MGDG). Each polar  
193 head group defines a phospholipid or glycolipid class, and each class can be divided into several  
194 molecular species according to the fatty acyl chain composition and distribution. When the fatty  
195 acyl chain structures are resolved but the sn-1 and sn-2 positions remain unclear, then the  
196 phospholipids or glycolipids are designated PL (C:n\_C:n), with C referring to the sum of the  
197 number of carbon atoms and n to the number of double bonds for each fatty acyl chain.

## 198 2.7. Conversion of phospholipids and glycolipids to fatty acid equivalents

199 Following the analysis of the different classes of polar lipids, and using the molecular  
200 species within each class, the different fatty acids were determined from the acyl chains  
201 previously identified. To this purpose, each mole of each molecular species was converted into  
202 its fatty acid equivalent.

203 Equation 1 1 mole of MGDG(16:3/18:3)  $\rightarrow$  1 mole of 16:3 + 1 mole of 18:3

204 Equation 2 1 mole of PG(18:1/18:1)  $\rightarrow$  2 moles of 18:1

205 Equation 1 illustrates the case where the acyl chains are asymmetric (i.e. the fatty acid at sn-1  
206 is different from that at sn-2), while Equation 2 corresponds to the case where two fatty acids  
207 with both the same numbers of carbons and unsaturations are present.

## 208 2.8. Data analyses

209 Data were processed using R 4.2.2 software (R Core Team, 2022) as well as Excel 2016  
210 with XLstat 2010 add-on statistical software. Each Principal Components Analysis (PCA) was  
211 performed with Pearson correlations. Non-parametric tests (Kruskal-Wallis) and multiple

212 comparison methods (Conover and Iman) were respectively carried out with a global p-value  
213  $\leq 0.05$  and Bonferroni corrections. Multivariate analysis of variance (MANOVA) and  
214 subsequent analysis of variance (ANOVA) were performed with Welch test corrections.

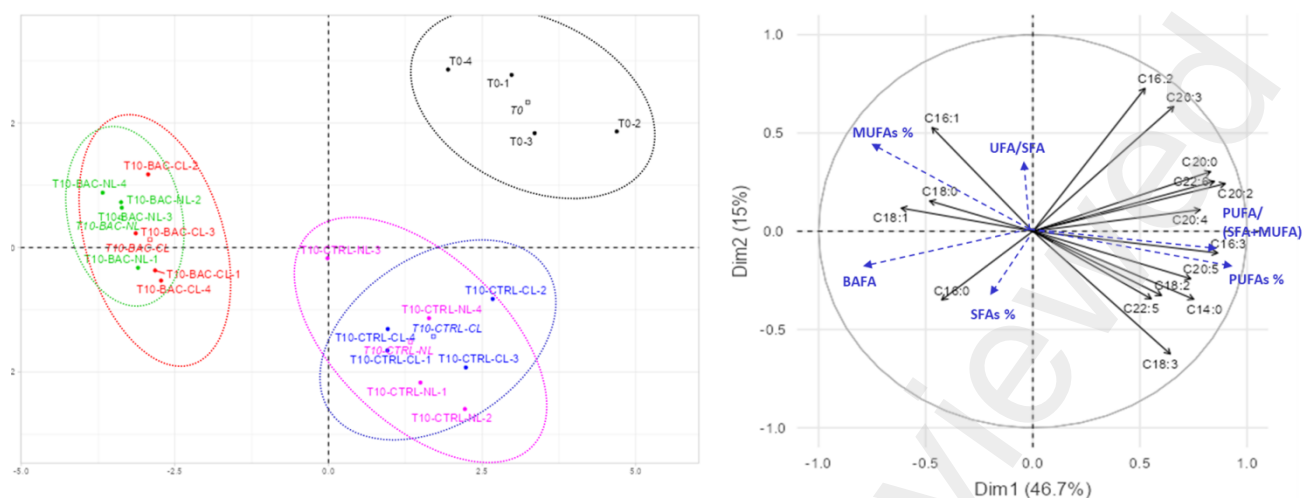
215

## 216 **3. Results**

217

### 218 **3.1. Fatty acids from polar lipids**

219 Fatty acids obtained from PG, PE, PC, MGDG and DGDG, as well as free fatty acids  
220 (FFA) (Table A 4), were plotted on a Principal Component Analysis (PCA) (Figure 1 and Figure  
221 A 1). It should be noted that FFA generally represented a small proportion with 3 to 12% of the  
222 total fatty acids quantified in the various sample extracts, regardless of the condition applied  
223 (Figure A 2). Polyunsaturated fatty acids (C16:3, C18:3, C20:2, C20:3, C20:4, C20:5, C22:5  
224 and C22:6) loaded along axis 1. These PUFAs appeared to be more abundant in the samples  
225 under CTRL conditions, both at the initial time (T0) and after 10 days of exposure. Conversely,  
226 two saturated fatty acids and monounsaturated fatty acids (16:1, 18:0 and 18:1) were most  
227 abundant after exposure to BAC12 for 10 days (Vrba et al. 2023). The second axis of the PCA  
228 only explained 15.0 % of the total inertia compared to 46.7 % for the first axis. This second  
229 axis did not allow for a clear discrimination of other factors, such as a possible effect of normal  
230 light (NL) or continuous light (CL) conditions. Another representation can be obtained with a  
231 combination of the second and the fourth axes (6.4 %), with however a consequent overlapping  
232 of the confidence intervals for T10 CTRL-NL and-CL samples (Figure A 1).



233

234 Figure 1. PCA (dimensions 1 and 2) with initial samples (T0), controls after 10 days (T10  
 235 CTRL) according to continuous (CL) or normal (NL) light, as well as samples contaminated  
 236 with BAC 12, after 10 days (T10 BAC) and also with the two light conditions (CL and NL).  
 237 The variables represented on the right correspond to fatty acids determined from polar lipids,  
 238 as well as free fatty acids. % SFAs, MUFAs and PUFAs as well as BAFA, UFA/SFA and  
 239 PUFA/(SFA+MUFA) ratios are represented as supplementary variables in blue.

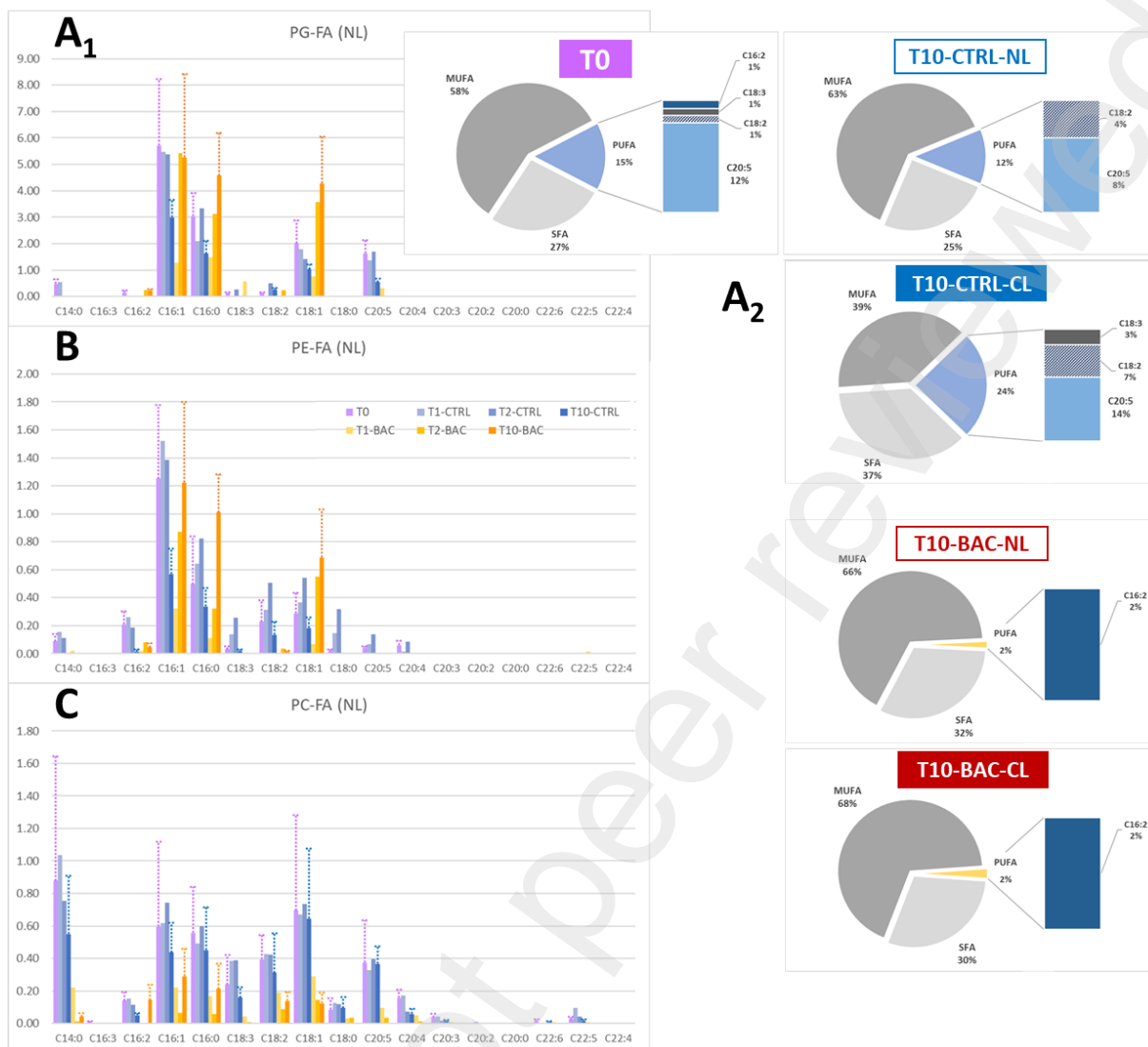
240

241 The amounts of fatty acids (in nmol mg<sup>-1</sup> of dry biofilm) obtained from the molecular  
 242 species of the phospholipids PG, PE and PC are presented in of Figure 2 (A1, B and C). These  
 243 barplots are presented only for the alternating photoperiod NL condition because the PCA  
 244 previously indicated that photoperiod did not markedly contribute to biofilm fatty acid  
 245 composition. The results presented in Figure 2 suggest a near disappearance of C20:5 within  
 246 PG, while C16:0, C16:1 and C18:1 highly increased in the presence of BAC 12. Panel A2  
 247 presents fatty acids from PG according to the categories SFAs, MUFAs and PUFAs. For the  
 248 uncontaminated controls, MUFAs seemed to be in the majority (58-63%) under normal light  
 249 condition at both T0 and T10. However, MUFAs appeared to be in equivalent proportion to  
 250 SFAs (39 and 37%, respectively) in the continuous light condition. PUFAs also seemed to  
 251 increase in the T10-CTRL-CL, however, this remains a trend as no significant differences were  
 252 found according to a non-parametric Kruskal-Wallis test. When considering either T10-BAC-  
 253 NL or CL samples a drastic decrease in PUFAs, essentially in favor of MUFAs, was observed

254 in the presence of BAC 12. It should be noted that C20:5, which composed the majority of the  
255 PUFAs in the CTRL samples, disappeared completely with exposure to the biocide.

256 The initial fatty acid composition (T0) from PE (Figure 2, panel B), as well as the  
257 composition after 2 and 10 days of experiment without BAC12 contamination, differed from  
258 that of PG where C18:2 and C18:3 were abundant and where C20:5 and C20:4 showed very  
259 low concentrations. Within the same phospholipids, and as observed for PG, an increase in  
260 MUFAs with 16 or 18 carbon atoms was observed, as well as the SFA C16:0. Finally, PC was  
261 characterized by an equivalent distribution of C18:2, C18:3 and C20:5 within the PUFAs from  
262 this class of membrane lipids, with contents essentially between 0.2 and 0.4 nmol mg<sup>-1</sup> (Figure  
263 2, panel C). We did not observe an increase in SFAs or MUFAs as a result of decreasing PUFAs.  
264 The results rather suggest that it is the fatty acids from PC that decreased in absolute values.

265



266

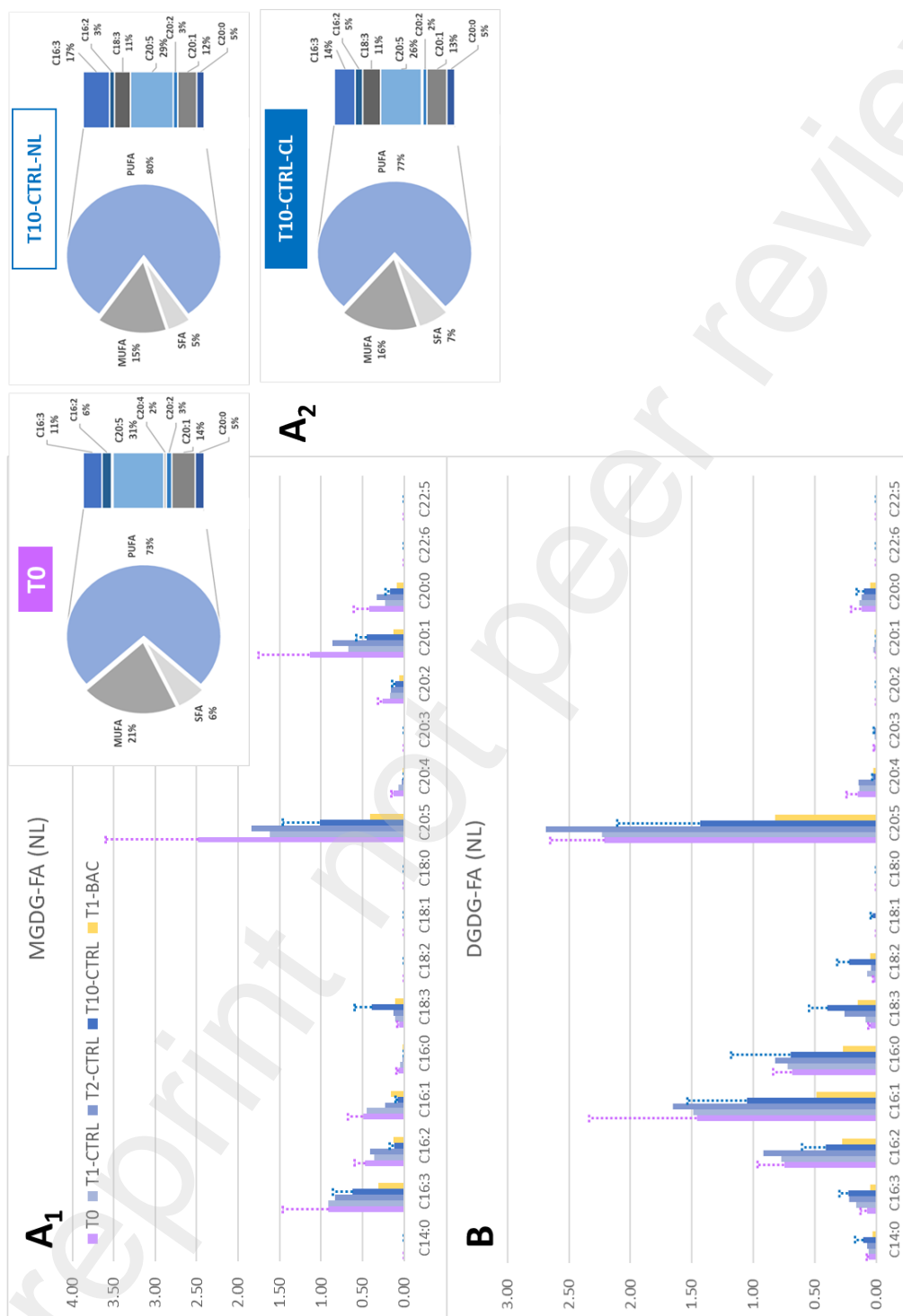
267 Figure 2. Evolution of fatty acids (nmol mg<sup>-1</sup>) deduced from the molecular species of  
 268 phospholipids (A1) PG, (B) PE and (C) PC. Different times are reported here with 1, 2 and 10  
 269 days of culture with or without BAC 12 and under normal light conditions. Part A2 on the right  
 270 illustrates for PG the grouping of fatty acids (% mol) within SFA, MUFA and PUFA, and then  
 271 the details for PUFAs only, for T0 and T10 samples.

272

273         Afterward, we considered the fatty acids associated with MGDG and DGDG. As  
 274 explained in Mazzella et al. (2023a), the method we used did not allow for the identification of  
 275 the acyl chains of SQDG, and therefore did not allow for an accurate determination of  
 276 associated fatty acids. Panels A1 and B of Figure 3 shows the evolution of the content of each  
 277 fatty acid within MGDG or DGDG. The most striking response was the near disappearance of  
 278 all fatty acids upon exposure to BAC 12, whatever the light conditions, and this was observed

279 from the first day. This may result from the sharp decline in MGDG and DGDG under those  
 280 same conditions, as previously observed in Vrba et al. (2023).

281



282  
 283 Figure 3. Evolution of fatty acid concentrations (nmol mg<sup>-1</sup>) calculated from the molecular  
 284 species of glycolipids (A1) MGDG, (B) DGDG. Panel A2 illustrates fatty acids (% mol)  
 285 within SFA, MUFA and PUFA for MGDG as well as individual PUFAs.

286

287 In the absence of contamination, C20:5 was the most abundant fatty acid in MGDG with  
288 both photoperiods (Figure 3, panel A2), followed by C16:3, C16:2 and C16:1 and long chain  
289 fatty acids such as C20:1 and C20:0. All fatty acids decreased over time with the exception of  
290 C18:3, which became more abundant at T10. Panel A2 of Figure 3 shows a noticeable stability  
291 in SFA, MUFA and PUFA after 10 days of growth in the artificial river channels. Looking at  
292 the relative proportions of each PUFAs, we could see a clear increase in C18:3 at the final  
293 sampling time with a relative proportion of almost 11 % compared to less than 1 % at the initial  
294 time. The fatty acid composition of DGDG was quite distinct from that of MGDG, with a more  
295 abundant pool of 16-carbon fatty acids, particularly centered around C16:1. The SFA, MUFA  
296 and PUFA categories are not represented here, however they appeared rather similar with a  
297 clear majority of PUFAs, as well as an equally stable composition over time in the samples not  
298 exposed to BAC 12.

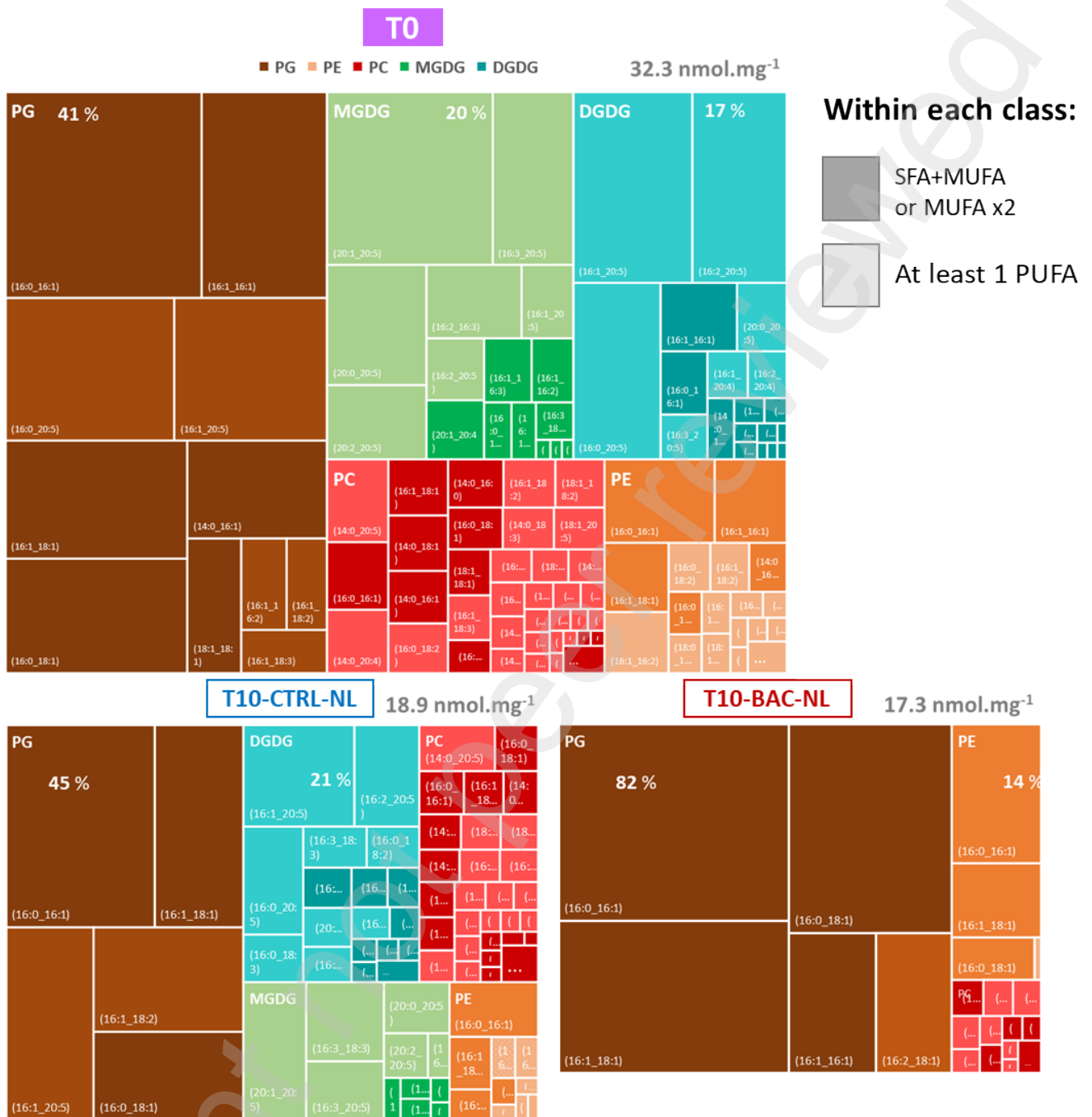
### 299 **3.2. Molecular species from polar lipids**

300 The molecular species identified within the main classes of PG, PE, PC, MGDG and  
301 DGDG are presented in Figure 4. The area of each rectangle is proportional to the relative  
302 amount in molar %. Only T0 and T10 under normal light conditions, with or without exposure  
303 to BAC 12, are shown. A very similar trend was observed under continuous light conditions  
304 and was consequently not illustrated here. At T0, PG clearly dominated with approximately  
305 41%, then MGDG and DGDG with 20 and 17%, respectively. These polar lipids are generally  
306 associated with thylakoid membranes in plants. Together, PC and PE represented less than a  
307 quarter of the polar lipids. These compounds are more representative of cytoplasmic  
308 membranes in plants. As with the fatty acids, we observed several molecular species containing  
309 at least one PUFA on each of the two acyl chains of each glycerolipid. In the case of PG, and  
310 especially MGDG and DGDG, we observed that most fatty acids were a combination between



311 eicosapentaenoic acid (EPA or C20:5) and a SFA or a MUFA such as C16:0, C16:1, C20:0 and  
312 C20:1. To a lesser extent, C20:5 appeared to be associated with C16:2 or C16:3.

313         After a 10-day exposure in the channels under normal light (T10-CTRL-NL), MGDG  
314 decreased in proportion comparable to DGDG and PC. Overall, we still observed many  
315 molecular species containing 1 or 2 PUFAs, but there was a slight increase in the representation  
316 of combinations between 16:3, 18:2 and 18:3 compared to the initial condition (T0). With the  
317 exposure to the biocide BAC 12 (T10-BAC-NL), we observed a radical change in both classes  
318 (i.e. MGDG and DGDG), with the general disappearance of the two glycolipids, as well as an  
319 apparent decrease in the number of compounds containing at least one PUFA. Thus, we were  
320 able to discern the presence of PG (16:0\_16:1), PG (16:0\_18:1) or PG (16:1\_18:1). The same  
321 applies to PE, the second most abundant phospholipid (PG and PE representing almost 96% of  
322 the initial polar lipids), with essentially mostly combinations between C16:0, C16:1 and C18:1.



323

324 Figure 4. Tree-map of molecular species, belonging to each of the polar lipid classes, detected  
 325 for samples at T0 and T10, contaminated or not with BAC, and for alternating/normal light  
 326 (NL) only. The surface of each block is proportional to the amount in nmol mg<sup>-1</sup>.

327

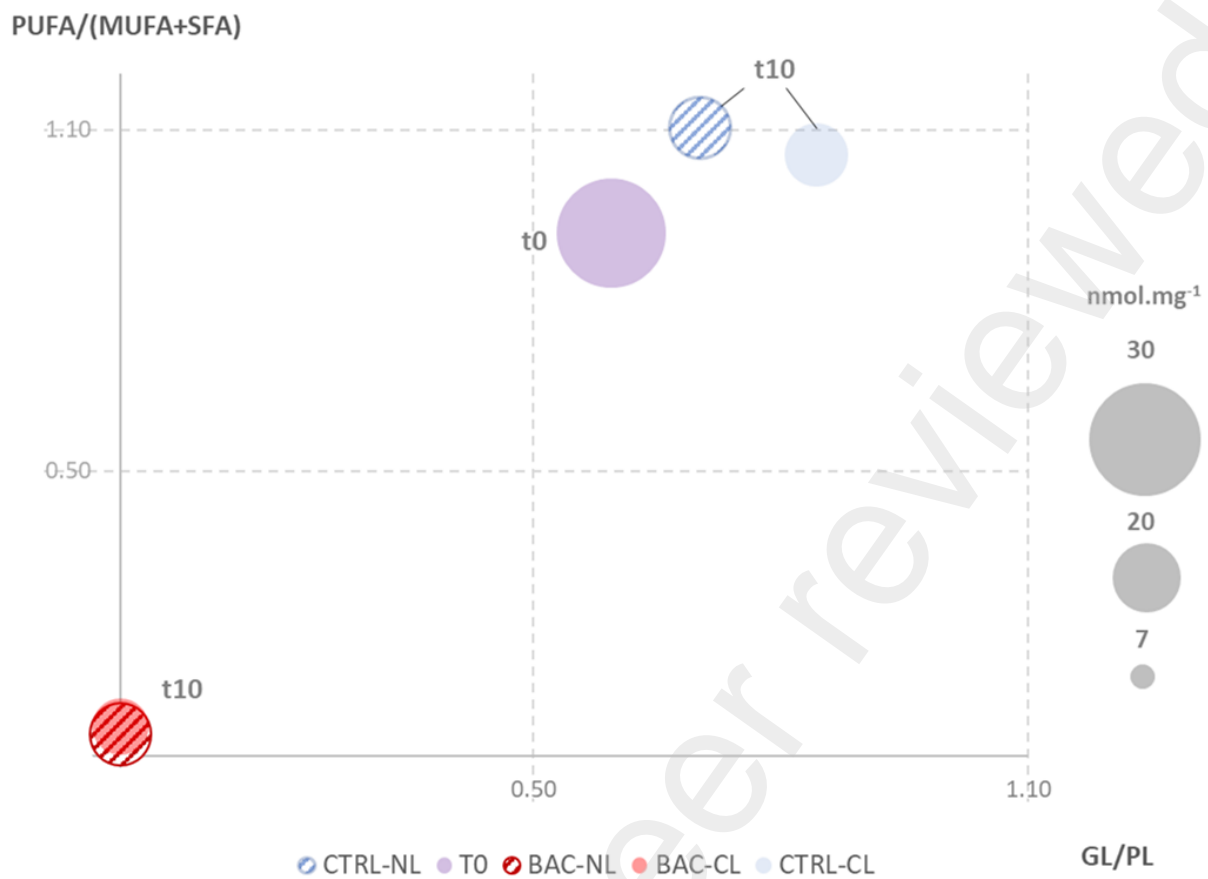
### 328 3.3. Covariation of polar lipid classes and fatty acid categories

329 A clear effect of BAC 12 on the evolution of both absolute and relative amounts of lipid

330 content in freshwater biofilms has been shown here at the fatty acid level, as previously reported

331 at the lipid class level in Vrba et al. (2023). For each date and condition, we have plotted on  
332 abscissa the ratio between the average amount of glycolipids (GL), represented here by all  
333 molecular species of MGDG and DGDG, and the average amount of phospholipids (PL) such  
334 as PG, PE and PC (i.e. GL/PL ratio). The ordinate is another ratio comprising all PUFAs (from  
335 all the classes) over the sum of the MUFAs and SFAs determined simultaneously in the same  
336 samples (i.e. (PUFA/(MUFA+SFA) ratio). In the top right-hand quadrant, for GL/PL and  
337 PUFA/(MUFA+SFA) ratios between 0.5 and 1.1, we can observe all the samples over the time,  
338 and whatever the photoperiod applied, corresponding to non-contaminated conditions. The  
339 unique and significant effect of BAC 12 was supported with a MANOVA for the two ratios  
340 (Table A 6). These are probably the highest values that the two indices can reach, indicating at  
341 the same time a proportion of PUFAs between one third and one half of all fatty acids, and a  
342 proportion of glycolipids between 30 and 40% of all polar lipids of both thylakoids and cell  
343 membranes. On the other hand, the lower left quadrant, with proportions that are both close to  
344 zero, i.e. the near disappearance of glycolipids and PUFAs, consists exclusively of samples  
345 contaminated with BAC 12. It should also be noted that the samples did not appear to be  
346 differentiated, whatever the light condition applied (NL or CL). These results suggested that  
347 PUFAs, even when considered as a whole, are essentially associated with glycolipids in this  
348 biofilm. In other words, the joint disappearance of MGDG and DGDG would lead to a  
349 consequent and sharp decrease in this category of fatty acids. The results of corresponding  
350 Welch's ANOVA was provided as supplementary information (Figure A 3).

351



352

353 Figure 5. Two-dimension scatter plot of samples over time, contaminated or not with BAC 12,  
 354 and with two light conditions. The size of the circle corresponds to the mean quantity of polar  
 355 lipids per sample and per condition.

356

357

## 4. Discussion

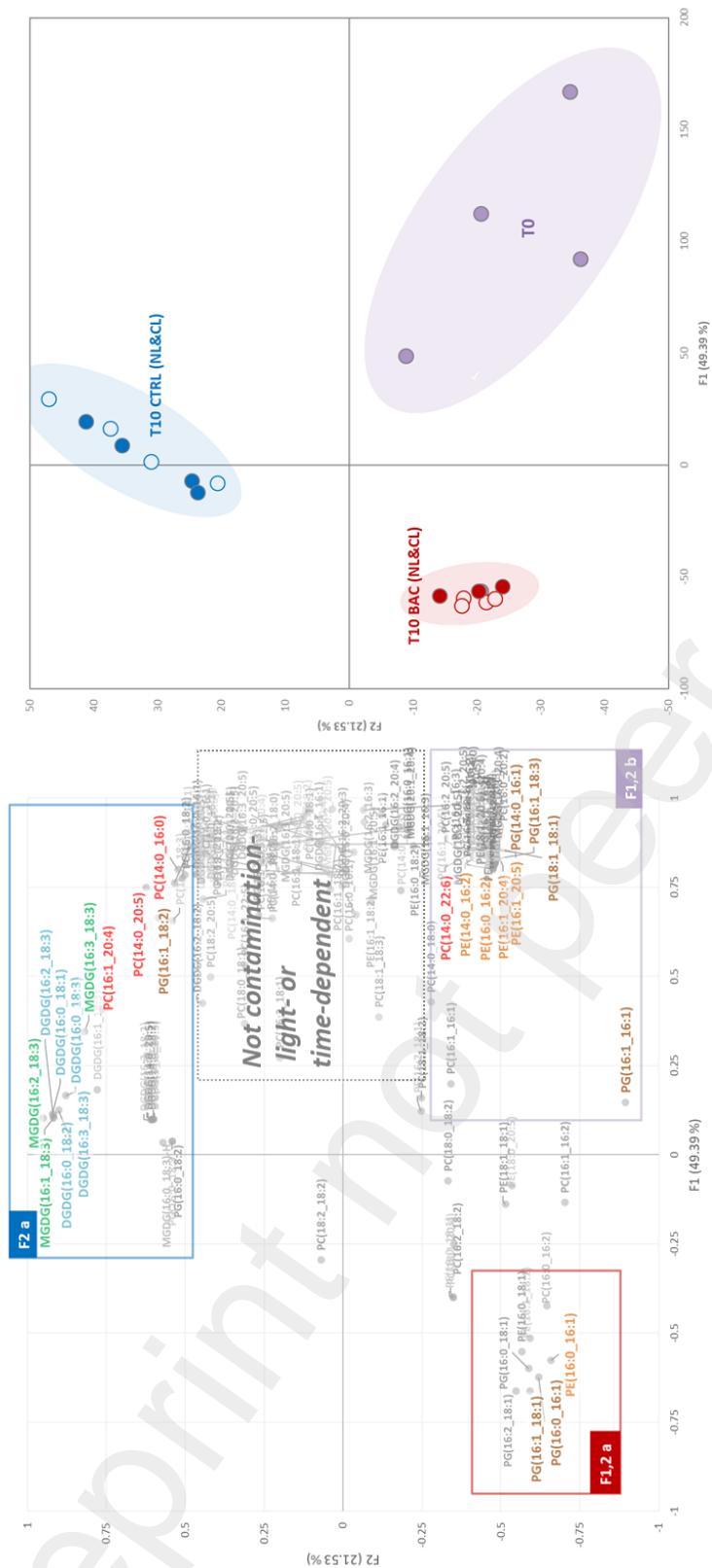
358  
359

### 4.1. BAC 12 effects over the time

361 The results presented in Figure 1, Figure 2 and Figure 3 showed that the samples  
362 contained polyunsaturated fatty acids in the absence of BAC 12, indicating that the biofilms  
363 contained photoautotrophs belonging to the bacillariophyceae, chlorophyceae and  
364 cyanophyceae groups (Vestal and White 1989, Guschina and Harwood 2009). This was also  
365 confirmed by fluorimetry and microscopy analyses (Vrba et al. 2023). Bacterial FA (BAFA  
366 index) with the sum of some SFAs and MUFAs like C15:0, C15:1, C16:0, C17:0, C17:1, C18:0  
367 and C18:1n-7 (Napolitano 1999, Dalsgaard et al. 2003) can also be used to estimate the  
368 contribution of bacteria to the biofilm community. The projection of the BAFA index among  
369 the additional variables in the PCA (Figure 1) could indicate an increase of the heterotrophic  
370 compartment over the time, under BAC 12 exposure, at the detriment of phototrophic  
371 organisms. In Figure A 1, axis 4 seems to allow for the separation between the continuous and  
372 alternating light conditions only in the T10-CTRL samples. This subtle distinction seems to be  
373 attributed to C16:0 and C18:3, which contributed more markedly to the CL condition, whereas  
374 C18:1 and C18:2 contributed more markedly to the NL condition. However, certain of these  
375 fatty acids (i.e., C18:2 and C18:3) were also potentially impacted by the presence or absence of  
376 BAC12 and, therefore, it becomes difficult to clearly disentangle the two factors solely based  
377 on the fatty acid composition of the polar lipids. The disappearance of certain classes of lipids  
378 (e.g., MGDG and DGDG) during exposure to BAC 12 has already been observed in the  
379 previous work conducted by Vrba et al. (2023). The overall decrease in PUFAs observed here  
380 on the same samples, also suggests a drastic decrease of all phototrophic organisms within the  
381 biofilm. It should be noted that other contaminants such as S-metolachlor, diuron, nickel or  
382 copper also caused a significant decrease in PUFAs in microalgal cultures or biofilms compared

383 to other fatty acid categories (Filimonova et al. 2016, Demailly et al. 2019, Fadhlouli et al.  
384 2020).

385 An additional data treatment consisted in a PCA using the molecular species  
386 composition of MGDG, DGDG, PG, PE and PC, in order to better distinguish the likely effects  
387 of BAC12 and light condition at the algal group level. The variables described in the F1-F2  
388 plane of the PCA (Figure 6) were sorted according to their decreasing contribution to these two  
389 axes, including only those with  $\cos^2 > 0.7$  (Table 1). A clustering of these filtered variables was  
390 then performed using a k-means classification (Figure A 4), resulting into three “variable  
391 clusters”, namely F2a, F1,2a and F1,2b. A fourth cluster has been identified, but when projected  
392 onto the variable plot (Figure 6), it did not appear to provide any sample- or condition-specific  
393 information. Additionally, we attempted to reassign molecular species to different autotrophic  
394 groups based on information from the literature (Opute 1974, Dunstan et al. 1993, Bergé et al.  
395 1995, Lang et al. 2011, Coniglio et al. 2021, Mazzella et al. 2023a). For example, molecular  
396 species containing C14:0, C20:5 or C22:6 were preferentially related to diatoms. In contrast,  
397 compounds with C18:2 or C18:3 associated with another 16- or 18-C SFA or MUFA were  
398 preferentially linked to contributions from green algae or cyanobacteria. Finally, when the  
399 molecular species appeared to be non-specific to a particular microbial groups (e.g. associations  
400 primarily among C16:0, C16:1 and C18:1), we indicated that it was an undetermined origin.  
401 Actually, it is possible to find such molecular species in all eukaryotic algae (Guschina and  
402 Harwood 2006), in fungi (Bhatia et al. 1972) as well as in prokaryotic organisms (Zelles 1997,  
403 Doumenq et al. 1999, Mazzella et al. 2005, Mazzella et al. 2007, Sohlenkamp and Geiger 2015).



404

405 Figure 6. F1- F2 plan of the PCA with the initial samples (T0), the controls after 10 days (T10  
 406 CTRL) under continuous (CL) or alternating (NL) light, as well as the samples contaminated  
 407 with BAC 12 after 10 days (T10 BAC) under the two light conditions (CL and NL). The  
 408 variables shown on the left correspond to the set of molecular species associated with polar  
 409 lipids.

410 Table 1. Molecular species filtered from the PCA results, considering the 20% of variables  
 411 contributing the most to the F1 and F2 axes, as well as with a  $\cos^2 > 0.7$  for the sum F1+F2.  
 412 Three clusters of variables (F2a, F1,2a and b) were defined, and likely attributions of the  
 413 variables was proposed according to the fatty acid composition highlighted within the selected  
 414 molecular species.

Molecular species	Top 20 % contributions axis F1+F2	Cos <sup>2</sup> > 0.7 axis F1+F2	Correlation significance <sup>1</sup>	Variable clusters	Likely algal attributions
DGDG(16:0_18:1)	3.010	0.863	***	F2 a	N.D.
DGDG(16:0_18:2)	2.981	0.854	***	F2 a	Chloro+Cyano
DGDG(16:0_18:3)	2.766	0.802	***	F2 a	Chloro+Cyano
DGDG(16:2_18:3)	2.980	0.853	***	F2 a	Chloro+Cyano
DGDG(16:3_18:3)	2.888	0.830	***	F2 a	Chloro+Cyano
MGDG(16:1_18:3)	2.980	0.853	***	F2 a	Chloro+Cyano
MGDG(16:2_18:3)	3.203	0.916	***	F2 a	Chloro+Cyano
MGDG(16:3_18:3)	2.547	0.791	***	F2 a	Chloro+Cyano
PC(14:0_16:0)	1.940	0.911	***	F2 a	Diatoms
PC(14:0_20:5)	2.235	0.950	***	F2 a	Diatoms
PC(16:1_20:4)	2.300	0.747	*	F2 a	Diatoms
PG(16:1_18:2)	1.888	0.785	**	F2 a	Chloro+Cyano
PE(16:0_16:1)	2.038	0.768	**	F1,2 a	N.D.
PG(16:0_16:1)	1.945	0.773	**	F1,2 a	N.D.
PG(16:1_18:1)	1.902	0.789	***	F1,2 a	N.D.
PC(14:0_22:6)	1.962	0.990	*	F1,2 b	Diatoms
PE(16:0_16:2)	1.971	0.993	***	F1,2 b	Chloro+Cyano
PE(16:1_20:4)	1.962	0.989	***	F1,2 b	Chloro+Cyano
PE(16:1_20:5)	1.953	0.967	***	F1,2 b	Diatoms
PG(14:0_16:1)	1.949	0.977	***	F1,2 b	Diatoms
PG(16:1_16:1)	2.846	0.821	***	F1,2 b	N.D.
PE(14:0_16:2)	1.980	0.988	***	F1,2 b	Chloro+Cyano
PG(16:1_18:3)	1.882	0.924	*	F1,2 b	Chloro+Cyano
PG(18:1_18:1)	1.963	0.974	***	F1,2 b	N.D.

415 <sup>1</sup>p-value <0.05 (\*), <0.01 (\*\*), <0.001 (\*\*\*) for correlations with F1 or F2

416 Cluster F2a was associated with the T10 CTRL samples, regardless of the photoperiod  
 417 condition, while cluster F1,2b was associated with the initial samples at T0. Cluster F1,2b  
 418 seemed to be more strongly related to the exposure to BAC 12 during the entire 10 days of  
 419 exposure. This result suggests that the presence of such a biocide exerts a selective pressure on  
 420 the different microorganisms constituting the biofilm, with a progressive elimination of  
 421 microalgae in favor of fungi or prokaryotes (Sakagami et al. 1989). These findings observed at  
 422 the molecular species level thus confirm the conclusions drawn from the taxonomic  
 423 observations formulated by Vrba et al. (2023). We may thus propose some potential biomarkers  
 424 by grouping increasing response of PC molecular species such as (14:0\_16:0), (14:0\_20:5) and  
 425 (16:1\_20:4), assumed to be here diatom-originating, in samples not contaminated with BAC 12  
 426 (Figure 7). However, it would be interesting to investigate further the degree of specificity of



427 this type of response to a specific contaminant in benthic microalgae at the level of lipid  
428 molecular species, especially with axenic culture conditions.

429

430

431

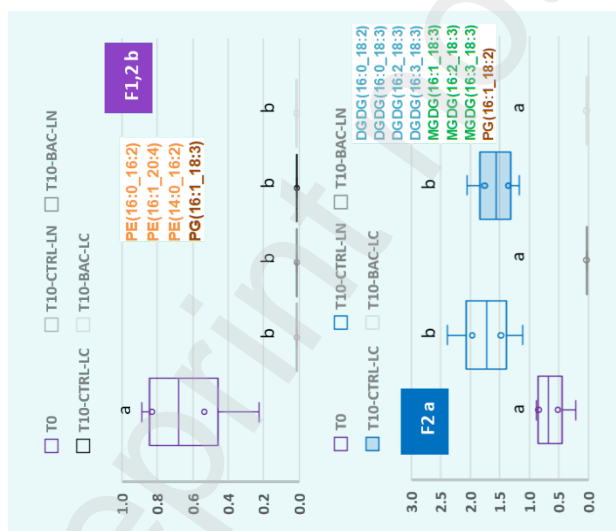
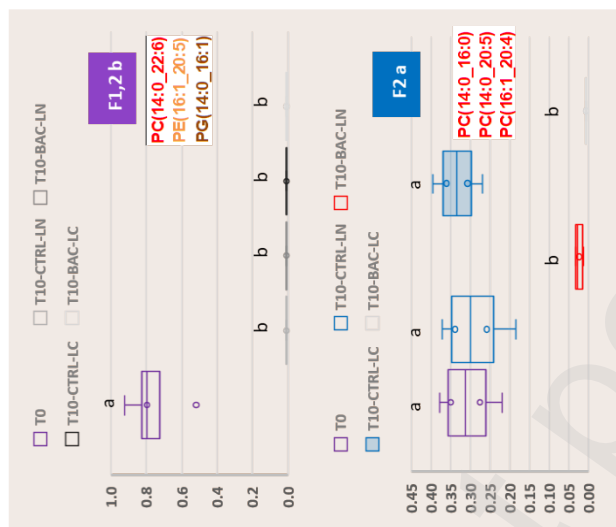
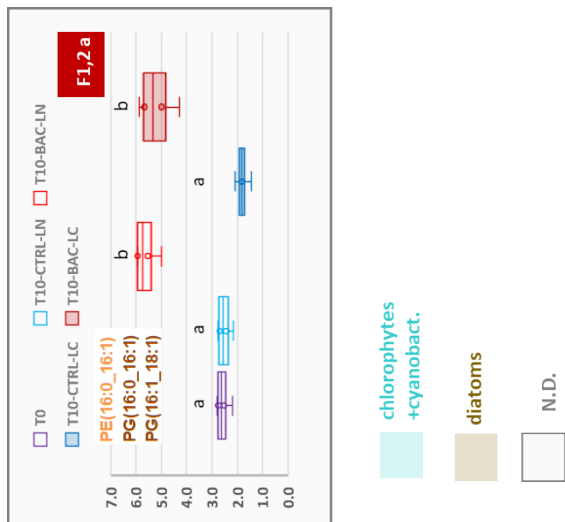
432

433

434

435

Preprint not peer reviewed

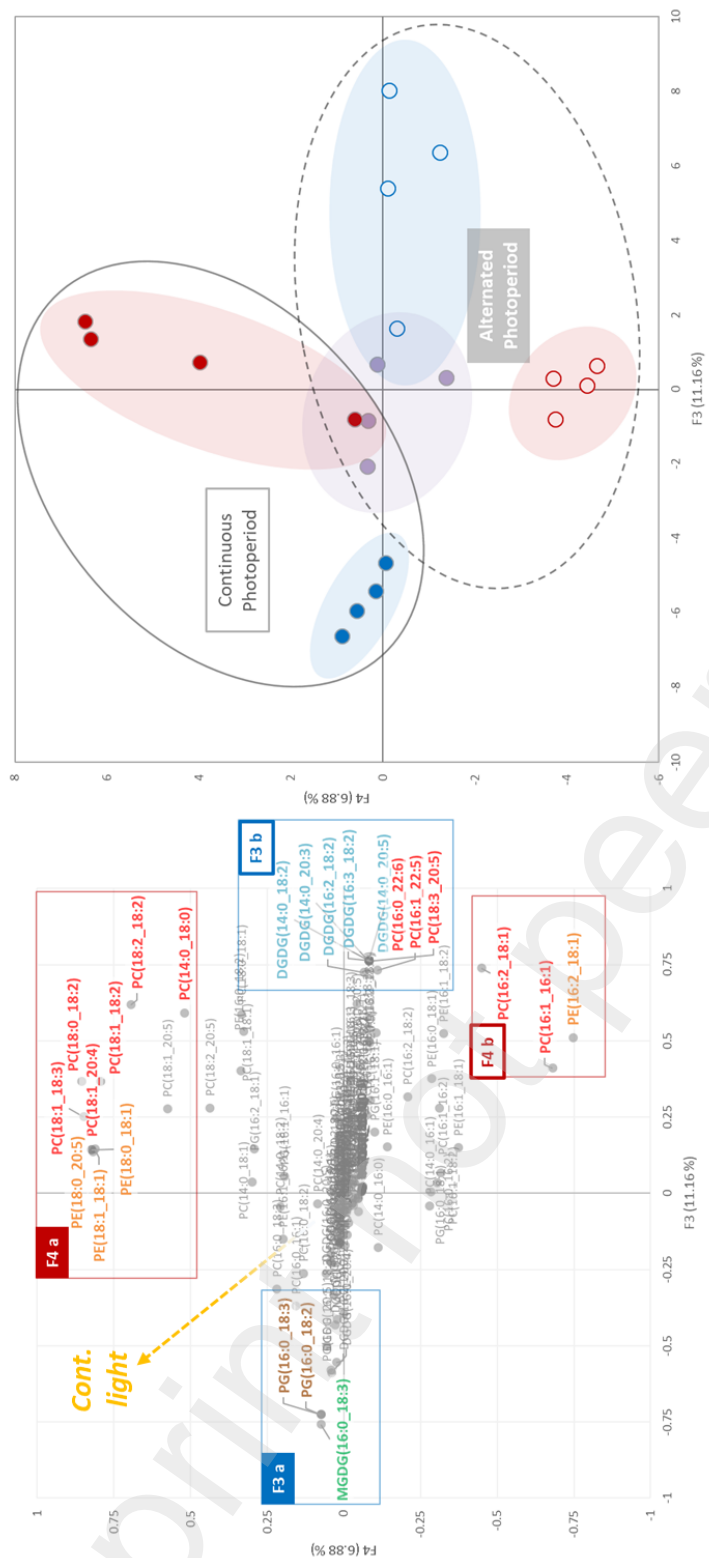


436

437 Figure 7. Variation of selected molecular species clusters (nmol mg<sup>-1</sup>) for each group of  
 438 variables (F2 a, F1,2 a and b) as a function of time (T0 or T10), BAC 12 (CTRL or BAC) as  
 439 well as the continuous or normal light conditions (CL or NL). The distinction was also made  
 440 based on the likely origin of the molecular species, according known and representative fatty  
 441 acids of certain autotroph groups.

#### 442 **4.2. Continuous versus alternated photoperiods**

443 No significant effect of the light condition (i.e., NL or CL) was observed on fatty acids  
444 derived from polar lipids. Vrba et al., 2023 came to the same conclusion based on analyses of  
445 the same samples at the level of lipid classes. This results in a difficulty to dissociate a possible  
446 effect of light condition from that of the contaminant. Because this study address also the  
447 molecular species, it is possible to keep information associated with the various fatty acids that  
448 can be attributed to specific microorganism groups from the biofilm. Actually, it become  
449 possible to attribute them either a phototrophic origin (i.e. PUFAs acyl chains of the MGDGs  
450 and DGDGs) or a heterotrophic origin (e.g. C16:0, C16:1 or C18:1 acyl chains of the PGs or  
451 PEs). Furthermore, in relation to light conditions, MGDG is thought to play an important role  
452 in the operation of the xanthophyll cycle in the thylakoid membranes of algae, including  
453 diatoms (Goss and Jakob 2010). MGDG is also present in cyanobacteria, the ancestors of  
454 chloroplasts in other photosynthetic organisms, even if the prokaryotic thylakoids do not  
455 operate a xanthophyll cycle, as found in algae. In addition, the development of thylakoid  
456 membrane networks, and therefore an effective photosynthesis, depends on a coordinated  
457 biosynthesis of thylakoid lipids with chlorophylls and photosynthetic proteins during  
458 chloroplast biogenesis, and both MGDG and DGDG plays a key-role during these processes  
459 (Wada and Murata 1998).



460

461 Figure 8 F3- F4 planes of the PCA with the initial samples (T0), the controls after 10 days (T10  
 462 CTRL) under continuous (CL) or normal (NL) light, as well as the samples contaminated with  
 463 BAC 12 after 10 days (T10 BAC) under the two light conditions (CL and NL). The variables  
 464 shown on the left correspond to the set of molecular species associated with polar lipids. The  
 465 continuous light vector is a supplementary variable.

466

467 Focusing on F3 and F4 axes of the PCA, a more specific discrimination related to the  
468 photoperiod was observed, as shown by the projection of this additional variable in the left part  
469 the graph (Figure 8). We then filtered the variables best represented in this F3-F4 plane of the  
470 PCA (Table 2) and defined four clusters (Figure A 4), as well as the probable assignment to  
471 specific algal groups. It is interesting to note that this analysis allowed the distinction between  
472 the samples that have undergone a continuous photoperiod from those that have been treated  
473 with an alternating photoperiod, as they appeared to be separated according to the first bisector  
474 associated with axes 3 and 4. Thus, the presence or absence of BAC 12 under the NL condition  
475 (i.e. alternating photoperiod) was distinguished by the two clusters F3b and F4b. On the other  
476 hand, the presence or absence of BAC 12 resulted in two other clusters, F3a and F4a, which  
477 were more indicative of the CL condition. Moreover, according to this clustering of variables,  
478 it seems that the continuous photoperiod may induce a relative increase in molecular species  
479 associated with green algae and cyanobacteria to the detriment of those originating from  
480 diatoms. In other words, the change in lipid composition revealed by molecular species analysis  
481 indicated that the CL condition would promote the growth of certain photoautotroph groups  
482 over time, regardless of the contamination pressure. Wang and Jia (2020) studied the  
483 photoprotective mechanisms of *Nannochloropsis oceanica* in response to light, mainly from  
484 the point of view of lipid and fatty acid classes, in parallel with the study of pigment  
485 composition. These authors showed that at higher intensities, there was a fairly marked decrease  
486 in MGDG and DGDG, but also in phospholipids. They also observed a decrease in most of the  
487 fatty acids associated with polar lipids, but this did not appear to be specific to certain categories  
488 such as PUFAs. The notable difference with our study is that the authors conducted their  
489 experiment on an algae culture while we studied the response of biofilms. In addition, they  
490 increased light intensities from 50 to 500  $\mu\text{mol m}^{-2} \text{s}^{-1}$  (20  $\mu\text{mol m}^{-2} \text{s}^{-1}$  for our study) with a  
491 continuous photoperiod only.

492 Table 2. Molecular species filtered from PCA results considering 30% of variables contributing  
 493 the most to the plane described by F3 and F4, as well as with a  $\cos^2 > 0.5$  for the sum F3+F4.  
 494 Four clusters of variables (F3a and b, F4a and b) were defined, and likely attributions of the  
 495 variables was proposed according to the fatty acid composition highlighted within the selected  
 496 molecular species.

497

Molecular species	Top 30 % contributions axis F3+F4	$\cos^2 > 0.5$ axis F3+F4	Correlation significance <sup>1</sup>	Variable clusters	Likely algal attributions
PG(16:0_18:2)	3.648	0.534	***	F3 a	Chloro+Cyano
PG(16:0_18:3)	3.648	0.534	***	F3 a	Chloro+Cyano
MGDG(16:0_18:3)	3.979	0.582	***	F3 a	Chloro+Cyano
PC(14:0_18:0)	5.355	0.619	**	F4 a	Diatoms
PC(18:0_18:2)	8.991	0.868	***	F4 a	Chloro+Cyano
PC(18:1_18:2)	7.840	0.763	***	F4 a	Chloro+Cyano
PC(18:1_18:3)	8.371	0.784	***	F4 a	Chloro+Cyano
PC(18:1_20:4)	7.614	0.699	***	F4 a	Diatoms
PC(18:2_18:2)	7.909	0.864	**	F4 a	Chloro+Cyano
PE(18:0_18:1)	7.606	0.698	**	F4 a	N.D.
PE(18:0_20:5)	7.505	0.689	***	F4 a	Diatoms
PE(18:1_18:1)	7.415	0.681	***	F4 a	N.D.
PC(16:0_22:6)	3.992	0.584	***	F3 b	Diatoms
PC(16:1_22:5)	3.751	0.545	***	F3 b	Diatoms
PC(18:3_20:5)	3.991	0.584	**	F3 b	Diatoms
DGDG(14:0_20:5)	4.017	0.587	***	F3 b	Diatoms
DGDG(14:0_18:2)	4.018	0.588	***	F3 b	Chloro+Cyano
DGDG(14:0_20:3)	4.011	0.587	*	F3 b	Diatoms
DGDG(16:2_18:2)	3.596	0.527	***	F3 b	Chloro+Cyano
DGDG(16:3_18:2)	4.026	0.589	***	F3 b	Chloro+Cyano
PC(16:1_16:1)	6.217	0.629	**	F4 b	N.D.
PC(16:2_18:1)	5.906	0.745	*	F4 b	Chloro+Cyano
PE(16:2_18:1)	7.895	0.816	***	F4 b	Chloro+Cyano

498 <sup>1</sup> p-value <0.05 (\*), <0.01 (\*\*), <0.001 (\*\*\*) for correlations with F3 or F4

499 The lipid content of algae is also significantly affected by light cycles. For example,  
 500 Brown et al. (1996) studied the effects of different light regimes on the lipids of the diatom  
 501 *Thalassiosira pseudonana* where 100, 50 and 100  $\mu\text{mol m}^{-2} \text{s}^{-1}$  under respective 12:12, 24:0 and  
 502 24:0 h light/dark cycles were used. Cells grown at the high light intensity and 12:12 photoperiod  
 503 exhibited higher concentrations of PUFAs and lower concentrations of both SFAs and MUFAs.  
 504 Although it is very likely that the duration of the photoperiod also affected the autotrophs found  
 505 in our biofilms, attributing changes to primary physiological effects at the level of each  
 506 individual organism in terms of fatty acid (or molecular species) content alone seems rather  
 507 uncertain. The change in lipid composition would appear here to be more closely tied to overall  
 508 changes in community structure because we investigated a complex biofilm. Fatty acids alone  
 509 may not provide sufficient information as they could, masking weaker effects like photoperiod

510 duration in favor of other environmental factors (i.e. simultaneous contamination exposure).  
511 Therefore, our suggestion is that some molecular species, especially those from PCs and  
512 DGDGs here (Table 2), may be more specific markers of light duration at a biofilm scale. In  
513 addition, the literature remains sparse at this level of molecular information, and we suggested  
514 to use similar lipidomic approach with monospecific cultures of microalgal strains to strengthen  
515 our preliminary results.

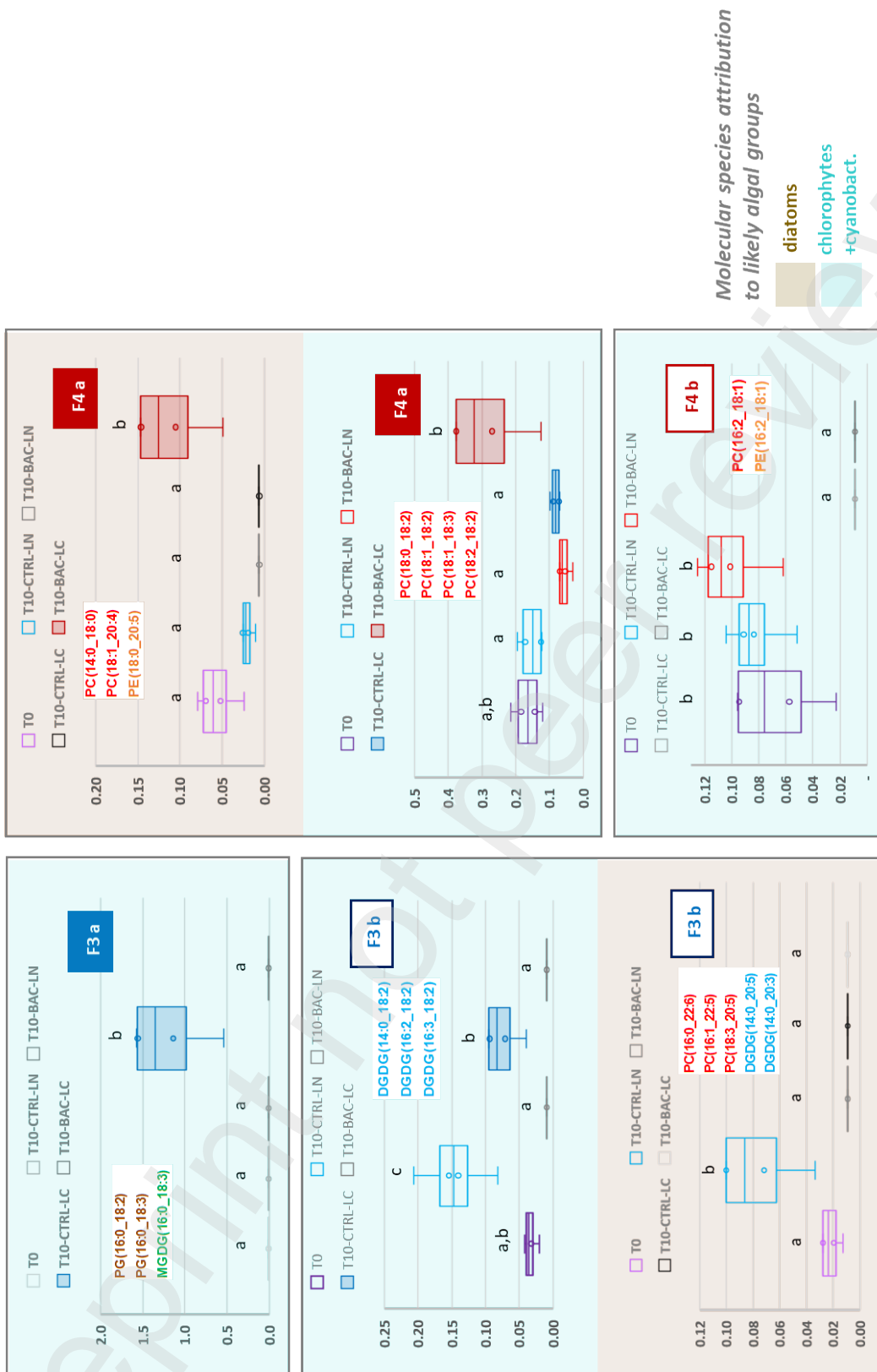
516

517

518

519

520



521 Figure 9. Variation of molecular species (nmol mg<sup>-1</sup>) clusters selected for each group of  
 522 variables (F3 a and b, F4 a and b) as a function of time (T0 or T10), BAC 12contamination  
 523 (CTRL or BAC) and light condition (CL or NL). The distinction was also made based on the  
 524 probable origin of the molecular species, according to the known and representative fatty acids  
 525 of certain photoautotroph groups.



## 526 **Conclusions**

527           After exposing biofilm to BAC 12, the fatty acid deduced from polar lipid analysis  
528 suggested that the heterotrophic compartment would likely increase at the expense of  
529 phototrophic organisms. The overall reduction in PUFAs found on the same samples points to  
530 a sharp decline in all phototrophic organisms present in the biofilm. To more clearly separate  
531 the co-occurring effects of biocide exposure and light condition at the algal group level, the  
532 molecular species compositions of MGDG, DGDG, PG, PE, and PC were examined. The most  
533 representative molecular species were clustered, and it was proposed that certain molecular  
534 species, particularly those from PCs and DGDGs, could potentially act as more accurate  
535 markers of light duration at the biofilm scale. To strengthen our early results, it would be  
536 beneficial to use a similar lipidomic approach with monospecific cultures of microalgal strains,  
537 since the literature is still lacking at this level of both molecular in-depth details and  
538 understanding of the physiological mechanisms.

539

540

541 **Author contributions**

542 Nicolas MAZZELLA: Lipid analysis, Data analysis, Writing - original draft, review & editing.

543 Romain VRBA: Conceptualization, Investigation, Methodology, Sample preparation

544 Aurélie MOREIRA: Lipid and micropollutant analyses

545 Nicolas CREUSOT: Writing - review & editing.

546 Mélissa EON: Sample preparation, Physico-chemical analysis

547 Débora MILLAN-NAVARRO: Physico-chemical and micropollutant analyses

548 Isabelle LAVOIE: Funding acquisition, Supervision, Writing - review & editing.

549 Soizic MORIN: Funding acquisition, Supervision, Conceptualization, Writing - review &  
550 editing.

551

552 **Conflicts of interest**

553 None

554

555 **Acknowledgements**

556 The authors would like to acknowledge the financial support from the Institut National de

557 Recherche pour l'Agriculture, l'alimentation et l'Environnement (INRAE) and l'Institut

558 National de la Recherche, Scientifique (INRS).

559

560

561

## 562 References

563

- 564 Arts, M. T., R. G. Ackman, and B. J. Holub. 2001. Essential fatty acids in aquatic ecosystems: a crucial  
565 link between diet and human health and evolution. *Can J Fish Aquat Sci* **58**:122–137.
- 566 Bergé, J.-P., J.-P. Gouygou, J.-P. Dubacq, and P. Durand. 1995. Reassessment of lipid composition of  
567 the diatom, *Skeletonema costatum*. *Phytochemistry* **39**:1017-1021.
- 568 Bhatia, I. S., R. K. Raheja, and D. S. Chahal. 1972. Fungal lipids. I. Effect of different nitrogen sources  
569 on the chemical composition. *Journal of the Science of Food and Agriculture* **23**:1197-1205.
- 570 Brown, M. R., G. A. Dunstan, S. J. Norwood, and K. A. Miller. 1996. Effects of harvest stage and light  
571 on the biochemical composition of the diatom *Thalassiosira pseudonana*. *Journal of Phycology*  
572 **32**:64-73.
- 573 Chaumet, B., S. Morin, O. Hourtané, J. Artigas, B. Delest, M. Eon, and N. Mazzella. 2019. Flow  
574 conditions influence diuron toxicokinetics and toxicodynamics in freshwater biofilms. *Science*  
575 *of The Total Environment* **652**:1242-1251.
- 576 Coniglio, D., M. Bianco, G. Ventura, C. D. Calvano, I. Losito, and T. R. I. Cataldi. 2021. Lipidomics of  
577 the Edible Brown Alga Wakame (*Undaria pinnatifida*) by Liquid Chromatography Coupled to  
578 Electrospray Ionization and Tandem Mass Spectrometry. *Molecules* **26**:4480.
- 579 Dalsgaard, J., M. St. John, G. Kattner, D. Müller-Navarra, and W. Hagen. 2003. Fatty acid trophic  
580 markers in the pelagic marine environment. Pages 225-340 *Advances in Marine Biology*.  
581 Academic Press.
- 582 Demailly, F., I. Elfeky, L. Malbezin, M. Le Guédard, M. Eon, J.-J. Bessoule, A. Feurtet-Mazel, F.  
583 Delmas, N. Mazzella, P. Gonzalez, and S. Morin. 2019. Impact of diuron and S-metolachlor on  
584 the freshwater diatom *Gomphonema gracile*: Complementarity between fatty acid profiles and  
585 different kinds of ecotoxicological impact-endpoints. *Science of The Total Environment*  
586 **688**:960-969.
- 587 Doumenq, P., M. Acquaviva, L. Asia, J. P. Durbec, Y. Le Dréau, G. Mille, and J. C. Bertrand. 1999.  
588 Changes in fatty acids of *Pseudomonas nautica*, a marine denitrifying bacterium, in response to  
589 n-eicosane as carbon source and various culture conditions. *FEMS Microbiology Ecology*  
590 **28**:151-161.
- 591 Dunstan, G. A., J. K. Volkman, S. M. Barrett, J.-M. Leroi, and S. W. Jeffrey. 1993. Essential  
592 polyunsaturated fatty acids from 14 species of diatom (Bacillariophyceae). *Phytochemistry*  
593 **35**:155-161.
- 594 Fadhlou, M., V. Laderriere, I. Lavoie, and C. Fortin. 2020. Influence of Temperature and Nickel on  
595 Algal Biofilm Fatty Acid Composition. *Environmental Toxicology and Chemistry* **39**:1566-  
596 1577.
- 597 Filimonova, V., F. Gonçalves, J. C. Marques, M. De Troch, and A. M. M. Gonçalves. 2016. Fatty acid  
598 profiling as bioindicator of chemical stress in marine organisms: A review. *Ecological*  
599 *Indicators* **67**:657-672.
- 600 Fuschino, J. R., I. A. Guschina, G. Dobson, N. D. Yan, J. L. Harwood, and M. T. Arts. 2011. Rising  
601 water temperatures alter lipid dynamics and reduce n-3 essential fatty acid concentrations in  
602 *Scenedesmus obliquus* (Chlorophyta). *J Phycol* **47**:763-774.
- 603 Goss, R., and T. Jakob. 2010. Regulation and function of xanthophyll cycle-dependent photoprotection  
604 in algae. *Photosynth Res* **106**:103–122.
- 605 Guschina, I. A., and J. L. Harwood. 2006. Lipids and lipid metabolism in eukaryotic algae. *Progress in*  
606 *Lipid Research* **45**:160-186.
- 607 Guschina, I. A., and J. L. Harwood. 2009. *Algal lipids and effect of the environment on their*  
608 *biochemistry*. Springer New York.
- 609 Lang, I., L. Hodac, T. Friedl, and I. Feussner. 2011. Fatty acid profiles and their distribution patterns in  
610 microalgae: a comprehensive analysis of more than 2000 strains from the SAG culture  
611 collection. *BMC plant biology* **11**:124-124.
- 612 Li-Beisson, Y., J. J. Thelen, E. Fedosejevs, and J. L. Harwood. 2019. The lipid biochemistry of  
613 eukaryotic algae. *Progress in Lipid Research* **74**:31-68.

- 614 Mazzella, N., M. Fadhlou, A. Moreira, and S. Morin. 2023a. Molecular species composition of polar  
615 lipids from two microalgae *Nitzschia palea* and *Scenedesmus costatus* using HPLC-ESI-  
616 MS/MS. ChemRxiv.
- 617 Mazzella, N., J. Molinet, A. D. Syakti, J.-C. Bertrand, and P. Doumenq. 2007. Assessment of the effects  
618 of hydrocarbon contamination on the sedimentary bacterial communities and determination of  
619 the polar lipid fraction purity: Relevance of intact phospholipid analysis. *Marine Chemistry*  
620 **103**:304-317.
- 621 Mazzella, N., J. Molinet, A. D. Syakti, A. Dodi, J.-C. Bertrand, and P. Doumenq. 2005. Use of  
622 electrospray ionization mass spectrometry for profiling of crude oil effects on the phospholipid  
623 molecular species of two marine bacteria. *Rapid Communications in Mass Spectrometry*  
624 **19**:3579-3588.
- 625 Mazzella, N., A. Moreira, M. Eon, A. Médina, D. Millan-Navarro, and N. Creusot. 2023b. Hydrophilic  
626 interaction liquid chromatography coupled with tandem mass spectrometry method for  
627 quantification of five phospholipid classes in various matrices. *MethodsX* **10**:102026.
- 628 Napolitano, G. E. 1999. Fatty Acids as Trophic and Chemical Markers in Freshwater Ecosystems. Pages  
629 21-44 in M. T. Arts and B. C. Wainman, editors. *Lipids in Freshwater Ecosystems*. Springer  
630 New York, New York, NY.
- 631 Opute, F. I. 1974. Lipid and Fatty-acid Composition of Diatoms. *Journal of Experimental Botany*  
632 **25**:823-835.
- 633 Robert, S., M. Mansour, and S. Blackburn. 2007. Metolachlor-Mediated Selection of a Microalgal Strain  
634 Producing Novel Polyunsaturated Fatty Acids. *Marine biotechnology (New York, N.Y.)* **9**:146-  
635 153.
- 636 Sakagami, Y., H. Yokoyama, H. Nishimura, Y. Ose, and T. Tashima. 1989. Mechanism of resistance to  
637 benzalkonium chloride by *Pseudomonas aeruginosa*. *Applied and Environmental Microbiology*  
638 **55**.
- 639 Sohlenkamp, C., and O. Geiger. 2015. Bacterial membrane lipids: diversity in structures and pathways.  
640 *FEMS Microbiology Reviews* **40**:133-159.
- 641 Vestal, J. R., and D. C. White. 1989. Lipid Analysis in Microbial Ecology: Quantitative approaches to  
642 the study of microbial communities. *BioScience* **39**:535-541.
- 643 Vrba, R., I. Lavoie, N. Creusot, M. Eon, D. Millan-Navarro, A. Feurtet-Mazel, N. Mazzella, A. Moreira,  
644 D. Planas, and S. Morin. 2023. Impacts of urban stressors on freshwater biofilms.  
645 bioRxiv:2023.2006.2011.544504.
- 646 Wacker, A., M. Piepho, and E. Spijkerman. 2015. Photosynthetic and fatty acid acclimation of four  
647 phytoplankton species in response to light intensity and phosphorus availability. *European*  
648 *Journal of Phycology* **50**:288-300.
- 649 Wada, H., and N. Murata. 1998. Membrane Lipids in Cyanobacteria. Pages 65-81 in S. Paul-André and  
650 M. Norio, editors. *Lipids in Photosynthesis: Structure, Function and Genetics*. Springer  
651 Netherlands, Dordrecht.
- 652 Wang, B., and J. Jia. 2020. Photoprotection mechanisms of *Nannochloropsis oceanica* in response to  
653 light stress. *Algal Research* **46**:101784.
- 654 Zäuner, S., W. Jochum, T. Bigorowski, and C. Benning. 2012. A cytochrome b5-containing plastid-  
655 located fatty acid desaturase from *Chlamydomonas reinhardtii*. *Eukaryot Cell* **11**:856-863.
- 656 Zelles, L. 1997. Phospholipid fatty acid profiles in selected members of soil microbial communities.  
657 *Chemosphere* **35**:275-294.
- 658 Zulu, N. N., K. Zienkiewicz, K. Vollheyde, and I. Feussner. 2018. Current trends to comprehend lipid  
659 metabolism in diatoms. *Progress in Lipid Research* **70**:1-16.

660

661

Preprint not peer reviewed

663 **Appendices**

664

665 Table A 1. BAC 12 concentrations (mg L<sup>-1</sup>) in the four experimental conditions at T10. BAC  
 666 12 = contaminated biofilm; CTRL = non-exposed biofilm; NL = alternated photoperiod; CL =  
 667 Continuous photoperiod.

Conditions	BAC 12 concentrations
T10-CTRL-NL	< 0.01
T10-BAC-NL	27.03 ± 12.12
T10-CTRL-CL	< 0.01
T10-BAC 12-CL	17.20 ± 7.47

668

669

670 Table A 2. Mass spectrometry parameters (single ion monitoring) for free fatty acid analysis.

671

Fatty acid	Q1 (m/z)	dwel time (ms)	DP (V)	CE (V)
C14:0	243	30	70	20
C15:0	257	30	70	20
C16:4	263	30	70	20
C16:3	265	30	70	20
C16:2	267	30	70	20
C16:1	269	30	70	20
C16:0	271	30	70	20
C17:1	283	30	70	20
C17:0	285	30	70	20
C18:4	291	30	70	20
C18:3	293	30	70	20
C18:2	295	30	70	20
C18:1	297	30	70	20
C18:0	299	30	70	20
C19:0	313	30	70	20

C20:5	317	30	70	20
C20:4	319	30	70	20
C20:1	325	30	70	20
C20:0	327	30	70	20
C22:6	343	30	70	20
C22:5	345	30	70	20

672

673

674 Table A 3. Chromatographic analytical gradient for free fatty acids separation.

<b>Time (min)</b>	<b>% of A (5 mM ammonium acetate)</b>	<b>% of B (acetonitrile:isopropanol, 50:50)</b>	<b>Flow rate (<math>\mu\text{L min}^{-1}</math>)</b>
0	50	50	300
0.3	50	50	300
5.8	1	99	300
8.8	1	99	300
9.1	50	50	300
11	50	50	300

675

676

677

678 Table A 4. Polar lipid-derived and free fatty acids data.

Polar + free FA C (nmol/mg)	T0				T10-CTRL-NL				T10-BAC-NL			
	rep1	rep2	rep3	rep4	rep1	rep2	rep3	rep4	rep1	rep2	rep3	rep4
C14:0	0.5	0.9	2.9	1.1	1.7	1.2	1.3	0.9	0.4	0.1	0.1	0.1
C16:3	1.6	0.9	1.4	1.2	0.8	1.3	0.4	1.1	-	-	-	-
C16:2	2.3	1.6	3.1	3.1	0.2	0.6	0.6	0.2	0.4	0.4	0.6	0.4
C16:1	15.9	3.2	9.5	15.8	4.2	1.7	11.8	6.0	9.7	4.9	8.7	8.2
C16:0	4.6	1.9	10.0	3.2	7.2	6.8	5.6	1.1	13.1	4.6	6.2	2.1
C18:3	0.6	0.3	1.0	0.9	1.7	1.4	0.8	0.5	-	-	-	-
C18:2	1.1	1.4	1.4	0.4	1.0	1.2	1.0	1.4	0.1	0.1	0.2	0.1
C18:1	2.7	2.1	0.9	3.5	2.3	2.2	2.6	2.5	0.7	0.6	4.6	9.2
C18:0	0.1	0.1	0.1	0.3	0.0	0.1	0.2	0.2	0.2	0.2	0.2	0.2
C20:5	1.2	6.2	1.9	3.8	1.1	1.8	3.3	4.0	-	-	-	-
C20:4	0.9	0.4	0.3	0.2	0.0	0.2	0.2	0.1	-	-	-	-
C20:3	0.1	0.0	0.1	0.1	0.0	0.0	0.0	0.0	-	-	-	-
C20:2	0.4	0.2	0.3	0.3	0.2	0.1	0.1	0.1	-	-	-	-
C20:0	1.6	1.0	2.2	0.9	0.3	0.3	0.1	0.2	-	-	-	-
C22:6	0.7	0.8	0.8	0.8	0.4	0.1	0.1	0.4	-	-	-	-
C22:5	0.0	-	-	0.1	-	0.0	0.0	0.0	-	-	-	-
Sum (nmol/mg)	34.0	20.8	35.9	35.6	21.0	18.9	28.2	18.5	24.5	10.8	20.6	20.2

SFAs (%)	20%	18%	42%	15%	44%	44%	26%	13%	56%	44%	32%	11%
MUFAs (%)	55%	25%	29%	54%	31%	21%	51%	46%	42%	51%	65%	86%
PUFAs (%)	26%	56%	28%	30%	26%	35%	23%	41%	2%	5%	4%	2%
PUFA/(SFA+MUFA) (%)	0.34	1.29	0.40	0.43	0.34	0.54	0.30	0.70	0.02	0.05	0.04	0.02
UFA/SFA (%)	4.04	4.44	1.36	5.51	1.29	1.25	2.91	6.62	0.80	1.25	2.17	7.76
BAFA (%)	21%	19%	31%	20%	45%	48%	30%	21%	57%	50%	54%	57%

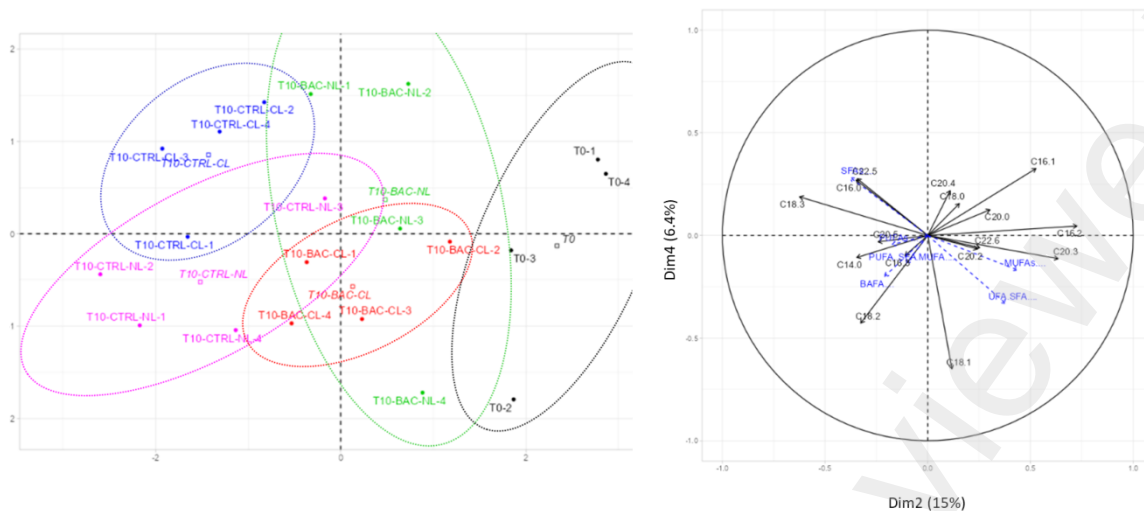
Polar + free FA C (nmol/mg)	T10-CTRL-CL				T10-BAC-CL			
	rep1	rep2	rep3	rep4	rep1	rep2	rep3	rep4
C14:0	1.3	0.7	0.9	0.9	0.1	0.2	0.1	0.1
C16:3	0.4	0.8	0.4	0.4	-	-	-	-
C16:2	0.8	0.7	0.5	0.3	0.5	0.5	0.2	0.6
C16:1	7.0	4.9	7.7	5.1	4.4	10.8	4.6	5.1
C16:0	6.1	4.8	3.2	5.6	7.6	1.4	3.0	9.8
C18:3	1.1	1.4	1.8	1.3	0.0	0.0	0.0	0.0
C18:2	1.3	0.4	1.3	0.0	0.6	0.5	0.2	0.5
C18:1	2.3	0.2	0.5	2.0	3.0	3.4	3.9	5.8
C18:0	0.1	0.1	0.1	0.1	0.2	0.1	0.1	0.0
C20:5	5.8	4.1	3.8	4.6	0.1	0.2	0.2	0.1
C20:4	0.3	0.3	0.3	0.3	0.0	0.0	0.0	0.0
C20:3	-	-	-	-	-	-	-	-
C20:2	0.2	0.1	0.2	0.0	-	-	-	-
C20:0	0.2	0.9	0.3	0.8	-	-	-	-
C22:6	-	0.5	0.2	0.4	-	-	-	-
C22:5	0.0	0.0	0.0	0.0	-	-	-	-
Sum (nmol/mg)	26.8	20.0	21.1	21.8	16.6	17.1	12.4	22.1

SFAs (%)	29%	32%	21%	34%	47%	10%	26%	45%
MUFAs (%)	35%	25%	39%	33%	45%	83%	68%	49%
PUFAs (%)	37%	42%	40%	34%	8%	7%	6%	6%
PUFA/(SFA+MUFA) (%)	0.58	0.73	0.67	0.50	0.08	0.07	0.06	0.06
UFA/SFA (%)	2.51	2.09	3.71	1.95	1.11	8.77	2.86	1.22
BAFA (%)	32%	26%	18%	35%	65%	29%	57%	71%

679

680

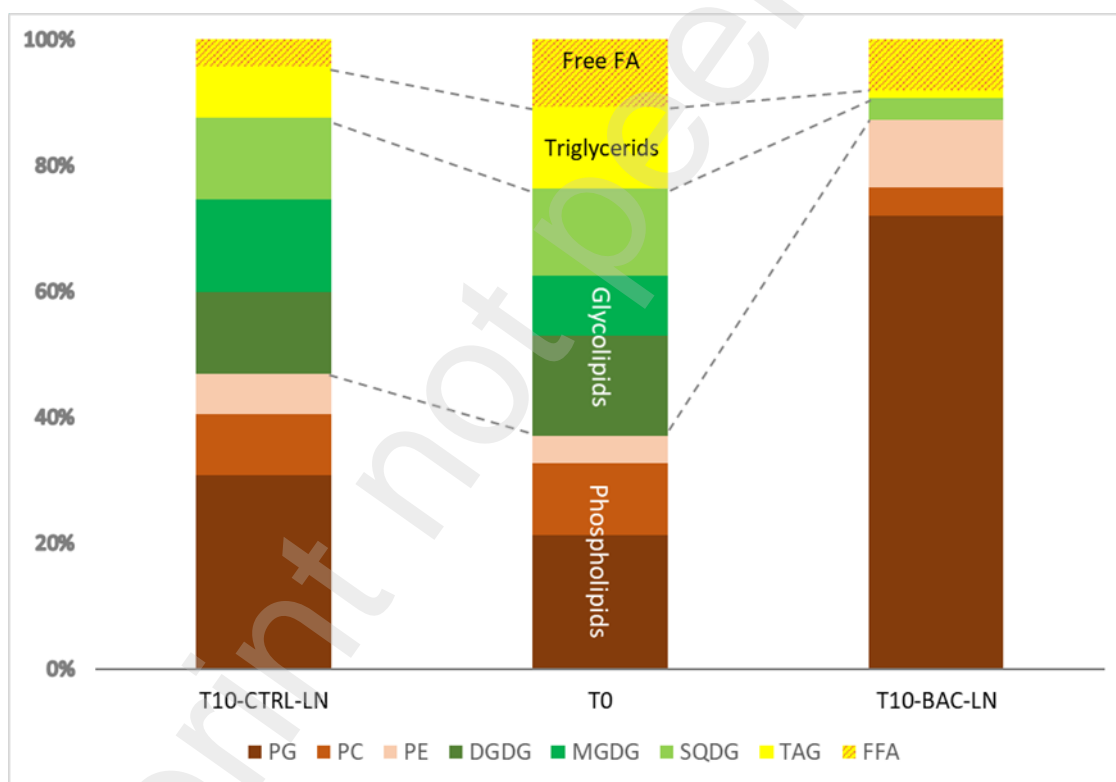




681

682 Figure A 1. Dimensions 2 and 4 of the PCA for fatty acids.

683



684

685 Figure A 2. Average lipid classes and FFA relative proportions.

686

687

688

689 Table A 5. Fatty acids as variables filtered by  $\cos^2$  values.

<b>Polar lipid FA</b>	<b><math>\cos^2 &gt; 0.5</math> (F1+F2)</b>
C20:0	<b>0.881</b>
C16:3	<b>0.875</b>
C16:2	<b>0.867</b>
C22:6	<b>0.807</b>
C20:5	<b>0.761</b>
C22:5	<b>0.752</b>
C20:4	<b>0.728</b>
C20:3	<b>0.727</b>
C18:3	0.615
C18:1	0.552
C20:2	0.545
C16:1	0.545
C18:0	0.522

690

691

692

693

694

695 Table A 6. Multivariate analysis of variance for both PUFA/(MUFA+SFA) and GL/PL ratios.

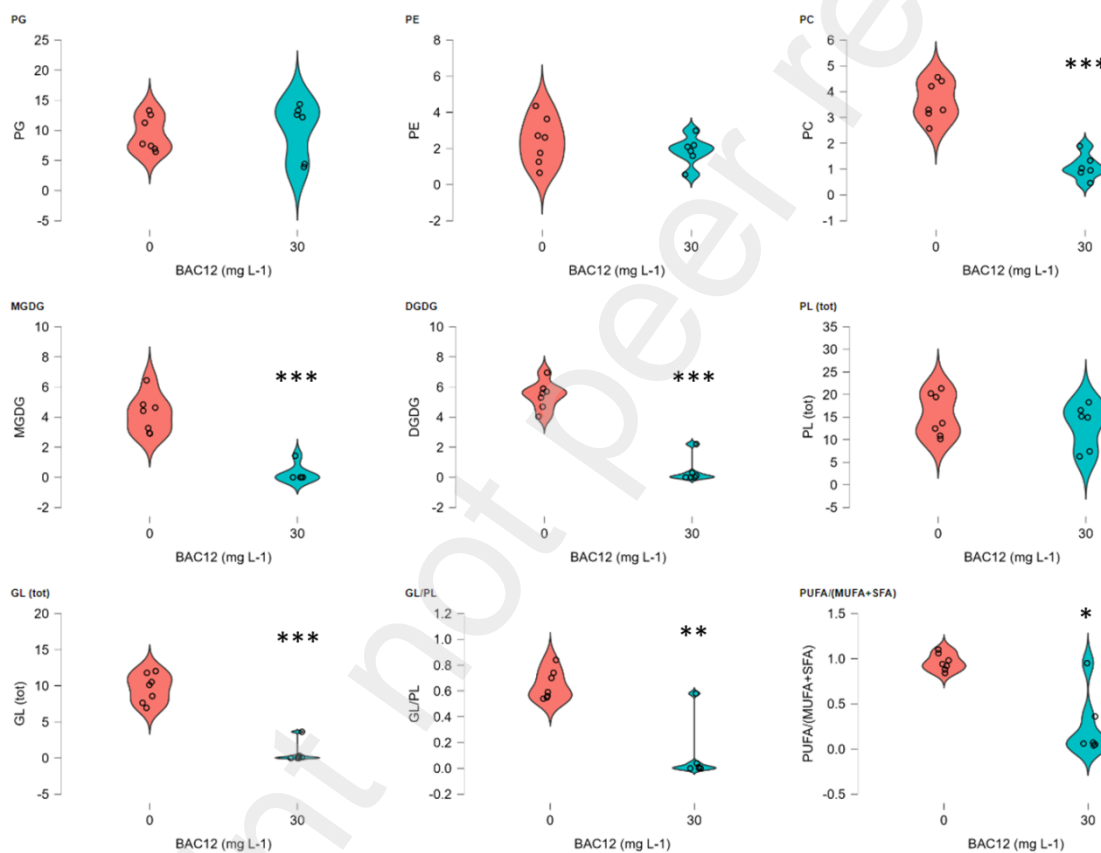
MANOVA

MANOVA: Pillai Test ▼

Cases	df	Approx. F	Trace <sub>Pillai</sub>	Num df	Den df	p
(Intercept)	1	32.123	0.889	2	8.000	1.504×10 <sup>-4</sup>
Light	1	0.977	0.196	2	8.000	0.417
BAC12 (mg L-1)	1	14.321	0.782	2	8.000	0.002
Light * BAC12 (mg L-1)	1	3.904	0.494	2	8.000	0.068
Residuals	9					

696

697

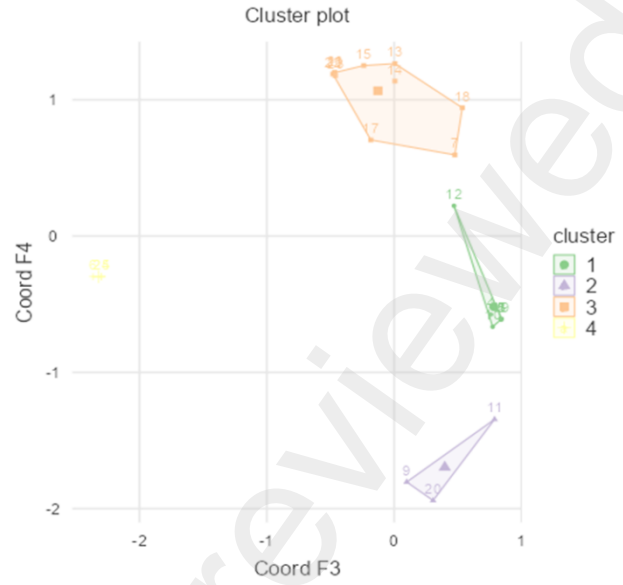
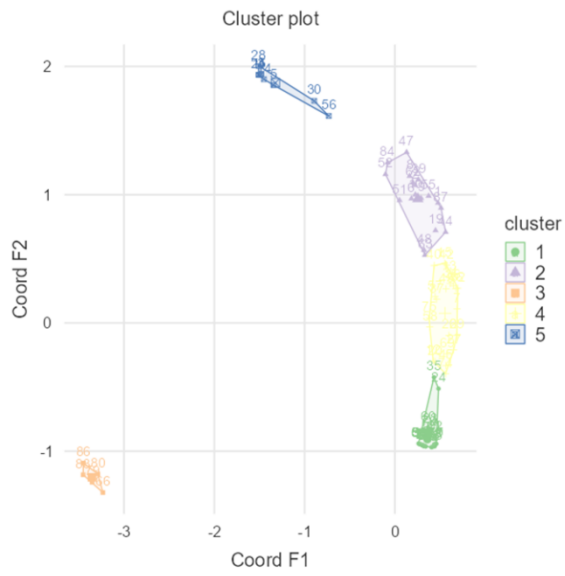


698

699 Figure A 3. Univariate (Welch's ANOVA) representation for each polar lipid class as well as  
 700 PUFA/(MUFA+SFA) and GL/PL ratios according to BAC 12 exposure. \* for p<0.05, \*\* for p<0.01,  
 701 \*\*\* for p<0.001.

702

703



704

705 Figure A 4. k-means clustering of variables best represented in either F1-F2 or F3-F4 plans.

706

707

708